

# 1 Concentrations and fluxes of isoprene and oxygenated VOCs at a 2 French Mediterranean oak forest

3 C. Kalogridis<sup>1</sup>, V. Gros<sup>1</sup>, R.Sarda-Esteve<sup>1</sup>, B. Langford<sup>2</sup>, B. Loubet<sup>3</sup>, B. Bonsang<sup>1</sup>, N.  
4 Bonnaire<sup>1</sup>, E. Nemitz<sup>2</sup>, A-C.Genard<sup>4</sup>, C. Boissard<sup>1</sup>, C. Fernandez<sup>4</sup>, E. Ormeño<sup>4</sup>, D.  
5 Baisnée<sup>1</sup>, I.Reiter<sup>5</sup> and J. Lathière<sup>1</sup>

6 [1]{Laboratoire des Sciences du Climat et de l'Environnement (LSCE-IPSL), Unité Mixte  
7 CEA-CNRS-UVSQ (Commissariat à l'Energie Atomique, Centre National de la Recherche  
8 Scientifique, Université de Versailles Saint-Quentin-en-Yvelines), F-91198 Gif-sur-Yvette,  
9 France.}

10 [2]{Centre for Ecology & Hydrology (CEH), Bush Estate, Penicuik, EH26 0QB, UK}

11 [3]{Environnement et Grandes Cultures, INRA, UMR EGC, Thiverval-Grignon, France}

12 [4]{Institut Méditerranéen d'Ecologie et Paléoécologie IMEP, 13397 Marseille, France}

13 [5]{Aix-Marseille Université, CNRS, ECCOREV FR 3098, Europôle de l'Arbois, 13545 Aix-  
14 en-Provence, France}

15 Correspondence to: V. Gros (valerie.gros@lsce.ipsl.fr)

16

## 17 **Abstract**

18 The CANOPEE project aims to better understand the biosphere-atmosphere exchanges of  
19 biogenic volatile organic compounds (BVOC) in the case of Mediterranean ecosystems and  
20 the impact of in-canopy processes on the atmospheric chemical composition above the  
21 canopy. Based on an intensive field campaign, the objective of our work was to determine the  
22 chemical composition of the air inside a canopy as well as the net fluxes of reactive species  
23 between the canopy and the boundary layer. Measurements were carried out during spring  
24 2012 at the field site of the Oak Observatory of the Observatoire de Haute Provence (O<sub>3</sub>HP)  
25 located in the southeast of France. The site is a forest ecosystem dominated by downy oak,  
26 *Quercus pubescens* Willd., a typical Mediterranean species which features large isoprene  
27 emission rates. Mixing ratios of isoprene, its degradation products methylvinylketone (MVK)  
28 and methacrolein (MACR) and several other oxygenated VOC (OxVOC) were measured  
29 above the canopy using an online proton transfer reaction mass spectrometer (PTR-MS), and

30 fluxes were calculated by the disjunct eddy covariance approach. The O<sub>3</sub>HP site was found to  
31 be a very significant source of isoprene emissions, with daily maximum ambient  
32 concentrations ranging between 2-16 ppbv inside and 2-5 ppbv just above the top of the forest  
33 canopy. Significant isoprene fluxes were observed only during daytime, following diurnal  
34 cycles with midday net emission fluxes from the canopy ranging between 2.0-9.7 mg m<sup>-2</sup> h<sup>-1</sup>.  
35 Net isoprene normalised flux (at 30 °C, 1000 μmol quanta m<sup>-2</sup> s<sup>-1</sup>) was estimated at 7.4 mg m<sup>-2</sup>  
36 h<sup>-1</sup>. Evidence of direct emission of methanol was also found exhibiting maximum daytime  
37 fluxes ranging between 0.2-0.6 mg m<sup>-2</sup> h<sup>-1</sup>, whereas flux values for monoterpenes and others  
38 OxVOC such as acetone and acetaldehyde were below the detection limit.  
39 The MVK+MACR-to-isoprene ratio provided useful information on the oxidation of isoprene,  
40 and is in agreement with recent findings proposing weak production yields of MVK and  
41 MACR, in remote forest regions where the NO<sub>x</sub> concentrations are low. In-canopy chemical  
42 oxidation of isoprene was found to be weak and did not seem to have a significant impact on  
43 isoprene concentrations and fluxes above the canopy.

44

## 45 **1 Introduction**

46 Volatile organic compounds (VOCs) are emitted into the atmosphere from natural sources  
47 (biogenic emissions) as well as from anthropogenic sources. Biogenic VOCs (BVOCs)  
48 constitute approximately 90% of global VOC emissions (Guenther et al., 1995). These  
49 emissions are characterized by a strong chemical diversity with more than a thousand BVOCs  
50 identified as emitted by plants. However, only a few of them contribute significantly to the  
51 global BVOC fluxes into the atmosphere (Laothawornkitkul et al., 2009). Isoprene (C<sub>5</sub>H<sub>8</sub>) is  
52 the most abundant BVOC in the Earth system, accounting for about half of all natural VOCs  
53 emitted at about 10<sup>15</sup> g(C) year<sup>-1</sup> (Guenther et al., 2012). Monoterpenes, sesquiterpenes but also  
54 oxygenated compounds, such as methanol, acetone and acetaldehyde may also be important  
55 regarding atmospheric chemical processes (Guenther et al., 1995; Kesselmeier et al., 1998;  
56 Kesselmeier J. and Staudt M., 1998; Fuentes et al., 2000; Park et al., 2013). Despite their  
57 relatively low atmospheric concentrations BVOCs are key components of tropospheric  
58 chemistry. Due to their high reactivity, they are rapidly oxidated by agents such as the OH  
59 radicals, thus significantly influencing the oxidizing capacity of the atmosphere and thereby  
60 impacting the residence time of air pollutants and the most reactive greenhouse gases such as  
61 methane (Wuebbles et al., 1989; Chiemchaisri et al., 2001). BVOCs also play a key role in the

62 tropospheric ozone cycle. In the presence of sufficiently high  $\text{NO}_x$  concentrations and light,  
63 BVOC emissions may be important precursors of regional-scale  $\text{O}_3$  (Trainer et al., 1987; Jacob  
64 and Wofsy, 1988; Chameides et al., 1988; Lee et al., 2006; Curci et al., 2010). As BVOC  
65 emissions increase with ambient light and temperature, the expected progression of climate  
66 change may impact BVOC emissions and contribute to regional  $\text{O}_3$  changes, but several  
67 processes still need to be better understood. BVOCs not only influence gas phase atmospheric  
68 chemistry; several studies have demonstrated that the oxidation of monoterpenes,  
69 sesquiterpenes, and, to a lesser extent, of isoprene, contributes to the formation of secondary  
70 organic aerosols (SOA) in the troposphere (Griffin et al., 1999; Claeys et al., 2004). The  
71 contribution estimate of BVOCs to SOA formation is still rather uncertain: Andreae and  
72 Crutzen, (1997) calculated this contribution to be in the range of 30-270  $\text{Tg yr}^{-1}$  whereas more  
73 recently Tsigaridis and Kanakidou (2003) estimated a smaller range of 2.5-44.5  $\text{Tg yr}^{-1}$ . These  
74 large uncertainties can be partly explained from the fact that current models use simplified  
75 SOA mechanisms that lump gaseous precursors and therefore lose information on the dry  
76 deposition removal of organic compounds which compete with the uptake of gases to the  
77 aerosol phase (Goldstein and Galbally, 2007; Hodzic et al., 2013).

78 In the Mediterranean region, the emissions and reactivity of BVOCs are enhanced due to high  
79 temperatures and sunny conditions and therefore are of particular interest for the production of  
80 SOA and  $\text{O}_3$ . A modelling study performed by Curci et al. (2010) predicts that, during summer  
81 in the Mediterranean region, BVOC emissions may be responsible for an increase of daily  $\text{O}_3$   
82 maxima by 5 ppbv, whereas Richards et al. (2013) estimated that a 20% cut in local BVOC  
83 emissions would lead to an average reduction of only 0.96 ppbv of  $\text{O}_3$  over the Mediterranean.

84 To evaluate the contribution of VOCs emitted by vegetation in the Mediterranean area to  $\text{O}_3$   
85 and SOA formation, a first step is to have accurate information on the amount of BVOCs  
86 released into the atmosphere. In this objective, we need to improve our knowledge regarding  
87 interactions between the terrestrial biosphere and the atmosphere. These interactions are still  
88 poorly understood and quantified. Several experimental studies demonstrated that a potential  
89 loss of BVOCs through chemical reactions and deposition inside the canopy could reduce the  
90 net fluxes into the atmosphere (Ciccioli et al., 1999). The loss of isoprene for example, within  
91 the canopy, could reach up to 40% (Makar et al., 1999). A few studies have also used  
92 Lagrangian-based stochastic model to explore the effect of chemical degradation of BVOCs  
93 inside the canopy (Strong et al., 2004; Rinne et al., 2012). Based on the Lagrangian approach  
94 along with measurements of oxidants on a Scots pine site, (Rinne et al., 2012) suggested that

95 in canopy-chemical degradation was negligible for isoprene but had a major effect on fluxes  
96 of most reactive species such as  $\beta$ -caryophyllene. Yet, those intra-canopy reactions are  
97 generally not considered in global vegetation or chemistry-transport models (Ciccioli et al.,  
98 1999; Makar et al., 1999; Fuentes et al., 2000; Forkel et al., 2006). Therefore, there is a need  
99 for more experimental data and analysis to quantify the impact of intra-canopy processes,  
100 together with a modelling approach in order to evaluate the related error in the estimates of  
101 net BVOC fluxes to the Mediterranean atmosphere.

102 A few studies have determined biogenic net emissions from Mediterranean ecosystems  
103 (Seufert et al., 1997; Ciccioli et al., 1999; Darmais et al., 2000; Davison et al., 2009a). During  
104 the first BEMA experiment (Biogenic Emissions in the Mediterranean Area 1994) several  
105 field campaigns were carried out at the Castelporziano site located on the Mediterranean coast  
106 near Rome, with one of the aims being to study BVOC emission fluxes above various  
107 Mediterranean species (Velentini et al., 1997). Emissions from orange plantations have also  
108 been studied in Spain within the framework of the second BEMA project 1997, and have  
109 shown an important loss of very reactive compounds such as sesquiterpenes due to within-  
110 canopy removal (Ciccioli et al., 1999) contrary to the low chemical destruction on the less  
111 reactive monoterpenes (Darmais et al., 2000).

112 Among the different tree species that characterize Mediterranean ecosystems, *Quercus*  
113 *pubescens* Willd. is of particular interest because of its large spatial coverage (most important  
114 tree species covering 20% of the vegetated surface, i.e 260 000 ha, in the Provence-Alpes-  
115 Côte d'Azur region) and high isoprene emission potential. Keenan et al. (2009) estimated that  
116 the contribution of *Q. pubescens* to the total European isoprene emissions budget exceeded  
117 15% for the 1960–1990 periods. Only a very limited number of BVOC flux measurements  
118 were performed on a *Q. pubescens* ecosystem. Simon et al. (2005) measured fluxes during  
119 one day using an aerodynamic gradient method in the forest of Montmeyan, while Baghi et al.  
120 (2012) used the disjunct eddy covariance method at the Observatoire de Haute Provence, both  
121 studies focusing exclusively on isoprene.

122 The originality of the CANOPEE ANR-JCJC project is to combine field experiments (branch-  
123 scale to canopy-scale measurements), targeting a large variety of BVOCs over a *Q. pubescens*  
124 forest, with modelling. Experimental data and observations collected during the intensive  
125 field campaigns will eventually be used in a one-dimensional canopy-chemistry model  
126 CACHE (Forkel et al., 2006) and a regional chemistry-transport model, CHIMERE (Schmidt  
127 et al., 2001; Szopa et al., 2009). Through these models, both, the in-canopy processes and the

128 role of local forested areas on the atmospheric chemical composition are studied for the  
129 Mediterranean region.

130 Our work consisted in measuring ambient BVOCs inside and above the O<sub>3</sub>HP canopy during an  
131 intensive campaign (June 2012). The objectives of this work were (1) to identify and quantify  
132 the VOC species locally emitted at the Observatoire de Haute Provence, (2) describe the  
133 temporal variation of their mixing ratios, (3) assess net fluxes of BVOC from the canopy to the  
134 boundary layer and (4) to discuss the isoprene fluxes and isoprene potential loss due to in-  
135 canopy oxidation.

136

## 137 **2 Methodology**

### 138 **2.1 Site description and general strategy**

139 The Observatoire de Haute Provence is an astronomical observatory located in south-eastern  
140 France (5° 42' 44" E, +43° 55' 54" N) on a plateau at a height of about 650 m. The Oak  
141 Observatory at the Observatoire de Haute Provence (O<sub>3</sub>HP, <https://o3hp.obs-hp.fr>) is an  
142 experimental station dedicated to the observation of a deciduous oak ecosystem in relation to  
143 climate change. The site, is dominated by downy oak (*Q pubescens* Willd) and Montpellier  
144 maple (*Acer monspessulanum* L.) representing 75% and 25% respectively, of the foliar biomass  
145 of the overstory tree species. The trees are about 70 years old and of an average height of 5 m.  
146 Understory vegetation is dominated by European smokebush (*Cotinus coggyria* Scop.) and  
147 many thermophilic and xerophilic herbaceous and grass species. The average single-sided leaf  
148 area index (LAI) measured (LAI-2000, Li-Cor, Lincoln, NE, USA) in August 2010 is 2.4. The  
149 flux footprint at the site was estimated to vary between 60 m and 120 m for respectively low  
150 and strong wind conditions. The calculation of the footprint was computed online  
151 (<http://www.footprint.kljun.net/>) based on Kljun et al. (2004) .

152 The climate is Sub-Mediterranean with warm-to-hot, dry summers and mild-to-cool, wet  
153 winters. During the field campaign the daily maximum temperatures typically ranged between  
154 18 and 30 °C.

155 Monthly diurnal isoprene samplings have been conducted at the O<sub>3</sub>HP over an 11-month period  
156 in order to characterize seasonal variations of ambient air concentration. During an intensive  
157 field campaign from 4<sup>th</sup> to 16<sup>th</sup> June 2012, measurements of BVOC, NO<sub>x</sub> and ozone  
158 concentrations, as well as flux measurements of individual VOC species, were performed. In

159 addition to atmospheric measurements, BVOCs emission rates at the branch scale were  
160 measured using dedicated chambers, and are described in the companion paper (Genard et al.,  
161 2014).

## 162 **2.2 Monthly isoprene sampling on cartridges and GC-MS analysis**

163 Prior to the intensive field campaign, the seasonal variation of isoprene was followed inside the  
164 canopy. Air samples were collected on a monthly basis between May 2011 and December 2011  
165 and from April 2012 to June 2012. Air was collected onto cartridges using an autosampler  
166 (SASS, TERA Environnement, Croles, France). Commercially packed cartridges consisted of  
167 stainless-steel tubes filled with Tenax TA adsorbents. For a single sequence, twelve cartridges  
168 collected a volume of 700 mL of air during 2 h. The air entering the cartridge was filtered in  
169 order to eliminate any particulate matter. Each sampling tube was kept refrigerated at 4°C and  
170 analysed at the laboratory within a month. The GC-MS analysis system consisted of an  
171 automatic desorption system (ATD 300, TurboMatrix, Perkin Elmer), coupled to a GC (Varian  
172 Model 3800, Varian Inc., USA) linked to an Ion trap mass spectrometer from the same  
173 company. Blank cartridges were analysed every 3 or 5 samples and showed no significant  
174 levels of isoprene. An external multi-point calibration was performed by doping the adsorbent  
175 tubes with a VOC standard (National Physical Laboratory, Teddington, Middlesex, UK). The  
176 quantification limit was less than 140 pptv.

## 177 **2.3 Ambient air sampling system during the intensive field campaign**

178 Ambient air sampling was conducted at two different heights: 2 m above ground level (a.g.l.)  
179 inside the canopy, and above the top of the canopy at about 10 m. Both sampling inlets were  
180 slightly heated to about 1°C above ambient temperature with a thermocouple type K connected  
181 to a 12V power supply in order to prevent water condensation. The lines were protected from  
182 radiation and attached to a pump-up mast, situated at 30 m from the van where all instruments  
183 were housed.

184 At 2 m a.g.l, air was pulled through a 35 m Teflon line (PFA, 1/2" outside diameter 'OD' and  
185 3/8" inner diameter 'ID') at about 40 L/min. Side flows were taken from a manifolds at the end  
186 of the main line through thinner Teflon lines (PFA, 1/4" OD, 5/32" ID) and sub-sampled by a  
187 range of gas analysers (GC-FID, NO<sub>x</sub> and ozone analysers).

188 At 10 m a.g.l, air was pulled through a 45 m Teflon line (PTFE, 1/2'' OD, 3/8'' ID) at a higher  
189 flow ( $\sim 64 \text{ L min}^{-1}$ ) in order to maintain the turbulent flow (Reynolds number = 9440) needed  
190 to minimize signal attenuation. A proton transfer reaction mass spectrometer (PTR-MS) and a  
191  $\text{CO}_2/\text{H}_2\text{O}$  analyser (IRGA LI-7500, Li-Cor, Lincoln, NE, USA) sub-sampled continuously at a  
192 flow rate of  $80 \text{ mL min}^{-1}$  and  $5 \text{ L min}^{-1}$  respectively. The displacement between the inlet and  
193 the sonic anemometer (HS-50 Hz, Gill Instruments Ltd., Hampshire, UK) was about 20 cm  
194 horizontally and 5 cm vertically. The representation of the tilt angle of the sonic anemometer as  
195 a function of wind speed showed no significant disturbance from the air motion within the  
196 detection region of the anemometer.

## 197 **2.4 BVOC measurement using proton transfer reaction mass spectrometer**

### 198 **2.4.1 PTR-MS Operation**

199 Concentrations and fluxes of VOCs above the canopy were processed in the real time with a  
200 PTR-MS (serial number: 10-HS02 079, 2010, Ionicon Analytik, Innsbruck Austria), a  
201 technique which has been described in recent reviews (De Gouw and Warneke, 2006, Blake et  
202 al., 2009) and references therein. Briefly, the PTR-MS used was a high sensitivity Ionicon  
203 model. We operated the drift tube at 2.2 mbar pressure,  $60 \text{ }^\circ\text{C}$  temperature and 600 V voltage,  
204 to achieve an  $E/N$  ratio of approximately 132 Td ( $E$ : electric field strength [ $\text{V cm}^{-1}$ ],  $N$ : buffer  
205 gas number density [ $\text{molecule cm}^{-3}$ ];  $1 \text{ Td} = 10^{-17} \text{ V cm}^2$ ). The primary  $\text{H}_3\text{O}^+$  ion count  
206 assessed at  $m/z$  21 ranged between  $0.9 \times 10^7$ - $1.9 \times 10^7$  cps with a typically  $< 5\%$  contribution  
207 from the monitored first water cluster at  $m/z$  37 and  $< 4\%$  contribution from the oxygen  $\text{O}_2^+$  at  
208  $m/z$  32.

209 A first series of measurements in scan mode enabled us to browse a wide range of masses  
210 ( $m/z$  21-  $m/z$  206) and to set the PTR-MS measurement procedure for the rest of the field  
211 campaign. Above  $m/z$  93, the only significant signal observed was at  $m/z$  137.

212 The PTR-MS measurement procedure consisted of an hour-long sequence. In order to provide  
213 both flux data and information on the full VOC composition, the PTR-MS was automatically  
214 set to run continuously in 2 different modes: twice 25 min in flux mode and twice 5 min in  
215 scan mode during each hour. During the flux mode, 8 protonated target masses ( $m/z$  33, 45,  
216 59, 61, 69, 71, 87 and 137) were measured successively with a dwell time of 500 ms per  
217 mass, while the primary ion count ( $m/z$  21), the first water cluster ion count ( $m/z$  37) and the  
218 photon "dark counts" ( $m/z$  25) were all measured with a dwell time of 200 ms. This resulted

219 in a total cycle time of 4.6 s and a total of  $n \approx 326$  recorded values per 25-min flux period. The  
220 remaining 10 min of each hour were used to obtain basic concentration information across the  
221 mass spectrum (5 min), and to monitor the instrument background (5 min). The PTR-MS  
222 background for each mass was monitored by sampling zero air (Ionimed's GCU zero air  
223 generator) and was subtracted during post processing. As each scan mode was set to 5 min  
224 and to a dwell time of 500 ms, the mass range was limited to  $m/z$  21–93, in order to have at  
225 least 5 data points for each mass per cycle.

226 PTR-MS data were stored alongside those from the sonic anemometer, using a custom  
227 logging program written in LabVIEW (National Instruments, Austin, Texas, USA) as  
228 previously implemented by Langford et al., (2009).

#### 229 **2.4.2 Calibration and volume mixing ratios (VMR) calculations**

230 The PTR-MS was calibrated on the first and the last days of the field campaign using a Gas  
231 Calibration Unit (GCU, Ionimed Analytik GbmH, Innsbruck, Austria), a dynamic gas dilution  
232 system that provides defined and controllable concentrations of different VOC using VOC-  
233 free air produced from ambient air with the GCU catalyst (Singer et al., 2007). The  
234 commercial internal gas canister provided by Ionimed contained a mixture of 17 VOCs. The  
235 species used for the calibration were methanol (contributing to  $m/z$  33), acetaldehyde ( $m/z$   
236 45), acetone ( $m/z$  59), isoprene ( $m/z$  69), crotonaldehyde ( $m/z$  71), 2-butanone ( $m/z$  73),  
237 benzene ( $m/z$  79) toluene ( $m/z$  93) and  $\alpha$ -pinene ( $m/z$  137). The VOC concentrations in the  
238 standard gas were diluted (8 dilution steps) from an initial mixing ratio of 1 ppmv to a mixing  
239 ratio of 20 ppbv. Calibration coefficients, also called normalized sensitivities ( $S_{\text{norm}}$ ) were  
240 calculated for each atomic mass unit (amu,  $m/z$ ) using the approach of Taipale et al. (2008).  
241 As methylvinylketone (MVK) and methacrolein (MACR) were not included in the gas  
242 standard, we used the sensitivity of their structural isomer crotonaldehyde. The sensitivity of  
243  $\alpha$ -pinene was used for the sum of total monoterpenes. Sum of monoterpenes have been  
244 commonly quantified based on both molecular ion ( $m/z$  137) and fragment ions ( $m/z$  81). In  
245 this study, total monoterpenes were only calibrated against  $m/z$  137. As considerable  
246 monoterpene fragmentation is expected for an E/N ratio of 132 Td, the abundance of the  
247 molecular ion ( $m/z$  137) is expected to decline in favor of the fragment ions (dominant at  $m/z$   
248 81). Also, as fragmentation patterns are dependent on the different monoterpenes species  
249 present, the sensitivity of  $m/z$  137 can slightly change if the monoterpenes composition is  
250 variable (Misztal et al. 2013). Nevertheless, additional measurements performed with



251 cartridges have shown that  $\alpha$ -pinene was the dominant terpene ( $80\pm 13\%$ ) and therefore  
252 calculated sensitivity of total monoterpene from  $m/z$  137 is justified (see supplement).

253 The differences in sensitivities from the two PTR-MS calibrations were below 5% for the  
254 compounds most discussed in the paper (methanol, acetaldehyde, acetone, isoprene and MVK  
255 +MACR). Higher differences of 9.36%, 12.51% and 20.19% were observed for benzene,  
256 toluene and monoterpenes respectively.

257 The mean values of normalized sensitivities determined from both gas calibration are given in  
258 Table 1, together with the detection limits, calculated as two times the standard deviation of the  
259 normalized background counts when measuring from the catalytically converted 'zero' air. For  
260 methanol, instrument background counts were generally high and therefore the ambient  
261 measurement signal was relatively high as well. However, all data points for methanol, and also  
262 acetone exceeded the detection limit. Approximately 9% of  $m/z$  45, 15% of  $m/z$  71, 20% of  $m/z$   
263 73 and  $m/z$  75 and 35% of  $m/z$  61 data points were below the detection limits, usually found at  
264 night or just before sunrise. As the background counts of  $m/z$  137 was not measured in the scan  
265 mode, they were derived from the calibrations, when the instrument was zeroed with  
266 catalytically converted air. The dwell time on each mass was 2000 ms during the calibration  
267 (instead of 500 ms during ambient measurements), thus, the background at  $m/z$  137 might have  
268 been slightly underestimated. Ambient mixing ratios of monoterpenes followed at  $m/z$  137,  
269 ranged between 0-0.26 ppb and only 58 % of the data points exceeded the detection limits.

270 Various techniques for statistical analysis of data below the detection limits have been  
271 developed and used. Most of these methods have advantages and disadvantages. A simple  
272 approach, commonly used, consists in replacing values below the LOD, with one-half their  
273 respective detection limits (Clarke, 1998). However, this substitution method can result in bias,  
274 either high or low depending on the value substituted (Helsel and Hirsch, 1992). In this study,  
275 all the compounds were considered representative in their full dataset, and no datapoints have  
276 been removed or substituted.

### 277 **2.4.3 Identification of VOC and Mass Interferences**

278 Standard PTR-MS instruments operate with a unit mass resolution and therefore cannot easily  
279 distinguish isobaric molecules. Furthermore, the formation of cluster ions and fragmentation  
280 of product ions may complicate the interpretation of PTR-MS mass spectra.

281 Isoprene for example, can fragment in the PTR-MS instrument and yield  $m/z$  41. During this  
282 study, the fragmentation of isoprene in the PTR-MS instrument was small: more than 80%  
283 remained on the parent ion ( $m/z$  69). Considering that  $m/z$  69 to  $m/z$  41 ratio is constant (for a  
284 fixed E/N value), quantification of isoprene based on  $m/z$  69 should not be affected by  
285 fragmentation.

286 Isoprene can suffer from interferences with isomers such as furans (Christian et al., 2004).  
287 However, as the site is not impacted by significant sources of anthropogenic pollution,  
288 furanes interferences were expected to be negligible. Eventually, fragments of 2- and 3-  
289 methyl butanal and 2-methyl-3-buten-2-ol (MBO) can also contribute to the ion channel  $m/z$   
290 69. Despite the possibility of these multiple interferences at  $m/z$  69, an inter-comparison  
291 showed a good agreement between PTR-MS and GC-FID, with a difference within the  
292 uncertainty range of both instruments (see Sect. 2.7). Considering the magnitude of isoprene  
293 emissions, it is very unlikely that any interference were significant.

294 As the GC-FID system deployed during the field campaign was designed for measuring  
295 exclusively hydrocarbons, no intercomparison with the PTR-MS was possible for the  
296 compounds attributed to C<sub>2</sub>–C<sub>6</sub> OxVOC. For these compounds the discussion of potential  
297 interferences is therefore based on literature.

298 Methanol, detected at  $m/z$  33, is expected to exhibit only little fragmentation but can suffer  
299 from interferences with the oxygen isotope  $^{16}\text{O}^{17}\text{O}$  detected at the same mass (De Gouw and  
300 Warneke, 2007; Taipale et al., 2008). Minimal interferences are also expected at  $m/z$  45,  
301 which is attributed to acetaldehyde. Acetone and propanal are both detected at  $m/z$  59 in PTR-  
302 MS, but previous studies showed that the contribution from propanal is typically only small  
303 (0%–10%) (De Gouw and Warneke, 2006) and confined to urban and industrial areas; the  
304 measurement at  $m/z$  59 can therefore be regarded as a measurement of acetone. Signals at  $m/z$   
305 61 include mainly acetic acid and glycoaldehyde but can also suffer interferences from ethyl  
306 acetate fragments originated from industrial emissions (Christian et al., 2004; de Gouw and  
307 Warneke, 2007; Haase et al., 2012; Yuan et al., 2013). The isomers methylvinylketone  
308 (MVK) and metacrolein (MACR) were detected at the same mass-to-charge ratio,  $m/z$  71.  
309 Until recently, the  $\text{C}_4\text{H}_7\text{O}^+$  ions have been exclusively attributed to the sum of the former  
310 compounds (Blake et al., 2009; de Gouw and Warneke, 2007). New evidence suggests  
311 additional contribution from of other isoprene oxidation products, believed to be mostly  
312 organic hydroperoxides, that fragment at the same  $m/z$  ratio as the product ions of MVK and  
313 MACR, especially for low-NO<sub>x</sub> conditions (Liu et al., 2013). As isoprene hydroperoxides are

314 expected to have similar diurnal variability to MVK and MACR, it is particularly difficult to  
315 estimate the contribution of isoprene hydroperoxides to  $m/z$  71. Thus, we have to keep in  
316 mind that the concentration attributed to MACR and MVK might be slightly overestimated.  
317 Major contribution at mass channel  $m/z$  73 are expected to originate from methylethylketone  
318 and methylpropanal, whereas the signal at  $m/z$  75 could correspond to hydroxyacetone (Karl et  
319 al., 2007). However potential interferences have been previously reported from butanal at  $m/z$   
320 73 and butanol and propionic acid at  $m/z$  75 (De Gouw and Warneke, 2007; Karl et al., 2009)  
321 and no further investigation was made during this work to be able to quantify these potential  
322 interferences. Total monoterpenes can be detected predominantly on the parent  $m/z$  137 and the  
323 fragment  $m/z$  81 ions. In this study, monoterpenes concentrations were calculated based on the  
324  $m/z$  137 signal.

## 325 2.5 Flux Calculations

326 Flux measurements of individual VOC species were performed using the micrometeorological  
327 disjunct eddy covariance by mass-scanning (DEC-MS) method also referred to as virtual  
328 disjunct eddy covariance technique (vDEC). DEC-MS and the conventional eddy covariance  
329 (EC) method rely on the same principle, that is, when the boundary layer is fully turbulent, the  
330 net vertical transfer is due to eddies. The flux of each compound is therefore calculated using a  
331 covariance function between the vertical wind speed ( $w$ ) and the VOC mixing ratio ( $c$ ):

$$332 \quad F = \frac{1}{n} \sum_{i=1}^n w' \left( i - \frac{t_{lag}}{\Delta_{tw}} \right) * c'(i) \quad (1)$$

333 Where,  $w'$  ( $= w - \bar{w}$ ) and  $c'$  ( $= c - \bar{c}$ ) are the instantaneous fluctuations about the mean  
334 vertical wind and the mean VOC concentration respectively,  $n$  is the number of PTR-MS  
335 measurements during each 25-min averaging period (here,  $n=326$ ),  $t_{lag}$  is the variable lagtime  
336 that exists between wind and PTR-MS measurements resulting from the sample transit through  
337 the sampling line, and  $\Delta_{tw}$  is the sampling interval of the vertical wind velocity measurements  
338 (20 Hz = 0.05s).

339 Further details can be found in Rinne et al. (2001), Karl et al. (2002) and Langford et  
340 al. (2009). Output files from the logging program containing 30 min arrays of wind and PTR-  
341 MS data (25 min) were post-processed by an algorithm written in LabVIEW by Langford et  
342 al. (2009) in order to calculate the VOC fluxes. Each data row corresponding to a given VOC  
343 was converted to ppbv and to  $\text{g}\cdot\text{m}^{-3}$  using temperature and pressure values recorded at the site.

344 Next, each VOC concentration data ( $c$ ) was paired with the corresponding vertical wind  
345 velocity ( $w$ ). The lagtime between ( $w$ ) and ( $c$ ) resulting from the sample residence time in the  
346 sampling line was variable due to fluctuations of temperature and pressure. For each 25 min  
347 period, lagtime ( $t_{lag}$ ) was automatically determined for each compound using the maximum  
348 covariance method between the VOC concentration ( $c$ ) and the vertical wind speed ( $w$ )  
349 (Taipale et al., 2010). For isoprene, a maximum covariance typically occurred around  
350  $15 \pm 0.6$  s. Based on isoprene results, MVK+MACR maximum covariance was searched within  
351 a window between 14 s and 16 s. Due to its sticky nature, methanol showed slightly longer  
352 lag times with a mean value of  $16.2 \pm 1.4$  s. The experimental mean time lag of each compound  
353 was used as the default value when we didn't find a maximum in the covariance function. The  
354 post-processing algorithm also filtered out data which did not meet specific quality criteria: 1)  
355 VOC flux data recorded during periods of low turbulence. The lower limit of friction velocity  
356  $u_*$  was set to  $0.15 \text{ m s}^{-1}$ , a threshold commonly used in eddy covariance routine tests  
357 (Langford et al., 2010; Misztal et al., 2011). 2) VOC flux values below the detection limit.  
358 The detection limit was calculated as three times the standard deviation of the covariance for  
359  $t_{lag}$  far away from the true lag (+150-180 s) (Spirig et al., 2005). 3) Non stationary data. A  
360 stationary test, as suggested for the first time by Foken (1996), was applied where the 25 min  
361 flux was disaggregated into 5 min blocks and the average of these compared to the 25 min  
362 flux. When the difference ( $\Delta$ s) between the average of the 5 minute blocks and the 25 min  
363 flux was above 60%, data were considered as non-stationary. Time series where the fluxes  
364 differed between 30% and 60% were considered stationary, but of low quality. When the  
365 fluxes differed by less than 30%, the data were considered as high quality stationary data.  
366 In the current study, 30% of isoprene, 29% of methanol and 60% of MVK+MACR datapoints  
367 were rejected. Of the data that passed the quality assessment, more than 80% were ranked as  
368 high quality. More statistics about these tests are presented in Table 3.

369 BVOC fluxes were corrected for high-frequency losses using the following equation:

$$F_{non-attenuated} = F_m * f_c$$

$$= F_m * (1 + ((2\pi \times \tau \times n_m \times \bar{u}) / (z - d))^{\alpha}) \quad (2)$$

371 where  $F_m$  is the measured flux,  $F_{non-attenuated}$  is the non -attenuated flux, and  $f_c$  the  
372 correction factor (Horst, 1997; Davison et al., 2009b).  $f_c$  was calculated as a function of  $\tau$ , the  
373 response time of the PTR-MS (here 0.5 s),  $z$  the measurement height (10 m),  $d$  the  
374 displacement height ( $\frac{2}{3}h_c$ , where  $h_c$  is the canopy height), and  $\bar{u}$  the average wind speed at

375 the measurement height. For neutral and unstable stratification, the dimensionless frequency  
376 at the co-spectral maximum is  $n_m = 0.085$  and  $= 7/8$ . Over the whole measurement period,  
377 the attenuation correction ranged from 1.1% to 23%, with a mean value of 13%.  
378 Eventually, the error introduced by disjunct sampling was estimated by comparing sensible  
379 heat fluxes calculated from continuous data with sensible heat fluxes calculated from disjunct  
380 series. In order to simulate the disjunct sampling protocol on sensible heat data, a LabVIEW  
381 routine was used to average the wind and temperature data to match the sampling rate of the  
382 PTR-MS (2 Hz) and set the sampling interval to 4.6 s. The difference between EC and DEC  
383 heat fluxes was small, typically below 2%. Assuming similarity between the heat flux and our  
384 VOC flux, a 2% error was estimated and no additional corrections have been made on the  
385 VOC fluxes.

## 386 **2.6 VOC measurements by Gas Chromatography**

387 An automatic gas chromatograph (airmoVOC C2-C6, Chromatotec, Saint Antoine France)  
388 equipped with a flame ionisation detector (GC-FID) suitable for the measurement of light  
389 hydrocarbons, especially for isoprene, sampled at 2 m above ground. For every half-hour  
390 analysis, 250 mL of ambient air were drawn into the system via a stainless steel inlet line with a  
391 flow rate of  $18 \text{ mL min}^{-1}$  (air sample integrated over 10 min). The air sample passed first  
392 through a Nafion dryer in order to remove the humidity and then hydrocarbons were pre-  
393 concentrated on a trap filled with Carboxen, Carboxen B and Carbotrap C. The trap was  
394 cooled to  $-8 \text{ }^\circ\text{C}$  by a cell with Peltier unit during the sampling procedure. Then, the pre-  
395 concentrated air sample was thermally desorbed at  $220 \text{ }^\circ\text{C}$  and injected on-column into a metal  
396 capillary column (Porous Layer Open Tubular Column PLOT,  $\text{Al}_2\text{O}_3/\text{KCl}$ ; 0.53-mm inner  
397 diameter and 25-m length, Varian Inc) located inside the heated oven of the GC. The column  
398 temperature was programmed to maintain  $40 \text{ }^\circ\text{C}$ , and then to heat-up at a rate of  $20 \text{ }^\circ\text{C.min}^{-1}$  up  
399 to a final temperature of  $203 \text{ }^\circ\text{C}$ . Non-oxygenated  $\text{C}_2\text{--C}_6$  hydrocarbons (mainly isoprene during  
400 the measurements) were finally detected and quantified by a FID. A certified standard gas  
401 mixture (National Physical Laboratory, Teddington, Middlesex, UK) containing a mixture of 17  
402 VOC at about 4 ppbv, was used as calibration standard. A complete calibration was performed  
403 twice a week. Each calibration was repeated at least three times in order to test the repeatability  
404 of the measurement. Relative standard deviations for analysis of the calibration mixtures were  
405 in the range of 1–9%. The overall uncertainty was estimated to be better than 15%.

## 406 **2.7 GC-FID/PTR-MS isoprene field comparison**

407 An *in-situ* comparison was carried out during the campaign between isoprene measurements by  
408 GC-FID and PTR-MS. Both instruments sampled air from the same line at 2 m a.g.l. The GC-  
409 FID integrated air sample over 10 min every 30 min. By contrast, the PTR-MS sampled air  
410 continuously and followed isoprene at  $m/z$  69 with a dwell time of 500 ms and a total cycle  
411 analysis of about one min. Only samples for which the GC-FID sample trapping interval and  
412 the PTR-MS sample cycle overlapped were included and the PTR-MS measurement were  
413 averaged over the 10 min sampling integration of the GC-FID. As this exercise lasted 19 hours,  
414 in total 38 points were used for this intercomparison. Overall a very good correlation was  
415 observed between both instruments ( $R^2=0.92$ ), with 10% higher values for the GC-FID, a  
416 difference which is within the uncertainty range. The intercomparison highlighted an average  
417 offset of +0.3 ppbv for the PTR-MS during nighttime, which was not subtracted from the PTR-  
418 MS datapoints and may be due to interferences from other VOCs. This nighttime offset has to  
419 be kept in mind but remains small compared to the average daytime isoprene concentrations  
420 (2.09 ppbv).

## 421 **2.8 NO<sub>x</sub>, ozone and micrometeorological measurements**

422 Nitrogen oxides (NO<sub>x</sub>) and ozone concentrations were measured 2 m a.g.l. A flow of  
423 920 mL min<sup>-1</sup> was sub-sampled from the main line and directed to the NO<sub>x</sub> analyzer. Nitrogen  
424 oxides were monitored with a T200UP instrument (Teledyne Advanced Pollution  
425 Instrumentation, San Diego, California, USA) by ozone-induced chemi-luminescence. A 30-  
426 min span calibration was performed every day using a dynamic dilution calibrator (T700 UP,  
427 API, USA) equipped with a programmable NO generator. The span calibration was automated  
428 to run 15 minutes of zero air (produced by the zero air generator T701H, API) followed by 15  
429 minutes of NO measurements generated at 5 ppbv. A calibration at 10 ppbv of NO was  
430 performed once a week by measuring 30 minutes of zero air and 30 minutes of a certified  
431 standard gas mixture (Air Liquide, Cofrac certification).

432 Ozone was measured with an automatic ultraviolet absorption's analyzer API T400 (API, USA)  
433 which was calibrated prior to the field deployment with an internal ozone generator (IZS, API)  
434 and operated with a sample flow rate of approximately 740 mL min<sup>-1</sup>.

435 Meteorological parameters such as temperature and air humidity (CS215, Campbell Scientific,  
436 UK) as well as photosynthetically active radiation, PAR (LI-190, Li-Cor, Lincoln, NE, USA),

437 profiles inside the canopy were continuously monitored. The sonic anemometer (HS-50 Hz,  
438 Gill Instrument, Hampshire, UK) enabled the measurement of wind speed and direction and to  
439 calculate the friction velocity  $u^*$ .

440

## 441 **3 Results**

### 442 **3.1 Ambient isoprene seasonal variations**

443 Figure 1 depicts the diurnal and seasonal variations of ambient, in-canopy, isoprene  
444 concentrations at the O<sub>3</sub>HP from May 2011 until May 2012. One or two complete diurnal  
445 cycles were taken every month. Even if the values reported here are representative only for the  
446 specific sampling days, significant seasonal variations of isoprene concentration were observed  
447 and were in agreement with the dependency of isoprene emission as a function of ambient light  
448 and temperature (Guenther et al., 1993). As conditions have been warmer in springtime than in  
449 summertime, maximum isoprene concentrations have been observed at the end of May with a  
450 maximum value of 8 ppbv. Lower concentrations were measured on the 14<sup>th</sup> and 31<sup>st</sup> July  
451 (maximum values of 4-5 ppbv) followed by a new increase in the end of August (9.8 ppbv);  
452 concentrations then decreased during the autumn when the leaves of the downy oak were still  
453 persistent and no significant isoprene concentration above detection limit was detected after  
454 November.

### 455 **3.2 Air Chemical Regime**

456 During the campaign the O<sub>3</sub>HP site was typically under the influence of northerly wind regime.  
457 As depicted on Fig. 2, air masses were usually transported from the (north) western part of  
458 France and only some sparse events of southern winds occurred (5-7<sup>th</sup> June, 14-16<sup>th</sup> June). Very  
459 low NO levels (< 0.2 ppbv) were detected and no significant influence from anthropogenic NO<sub>x</sub>  
460 was observed (NO<sub>2</sub> < 3 ppbv). Likewise, CO concentrations were low throughout the study (<  
461 180 ppbv). Benzene and toluene measurements, detected and used as tracers of anthropogenic  
462 pollution, showed background levels below 0.2 ppbv with the exception of one brief episode  
463 (the 7<sup>th</sup> and 8<sup>th</sup> June) when their concentration reached 0.8 and 1.6 ppbv (Fig. 3). During this  
464 episode the benzene-to-toluene ratio was slightly lower than for the rest of the measurement  
465 period and ranged between 0.3-0.8, indicating an influence of fresh anthropogenic air masses.  
466 As benzene and toluene have different lifetimes, the higher the benzene-to-toluene ratio the

467 older is the air mass. Globally, the air masses encountered were not significantly impacted by  
468 anthropogenic primary emissions.

469 Relatively high ozone concentrations, typical of regions with strong photochemical activity  
470 such as the Mediterranean Basin, have been registered, with daily maximum ranging between  
471 40-76 ppb.”

### 472 **3.2.1 Isoprene Mixing Ratios and above-canopy fluxes**

473 The May-June 2012 time series of isoprene mixing ratios recorded simultaneously at 2 m  
474 (inside the canopy by GC-FID) and at 10 m height (above the canopy by PTR-MS) are shown  
475 in Fig. 3 along with air temperature and wind conditions. Isoprene exhibited high  
476 concentrations with an average mixing ratio of 1.2 ppbv above the canopy (Table 2). Among all  
477 observed VOCs, isoprene presented the largest amplitude between day and night time  
478 concentrations, this behaviour being typical of those biogenic compounds whose emissions are  
479 light and temperature dependent (Guenther et al., 1993; Goldstein et al., 1998). Night time  
480 isoprene concentrations were close to our detection limit and started to increase steadily early  
481 in the morning, around 6.30 a.m. in response to the temperature and PAR increase. Maximum  
482 concentrations occurred in the afternoon, peaking between 2.0-5.0 ppbv and 2.0-16.9 ppbv at  
483 10 m and 2 m heights, respectively. In comparison, maximum atmospheric mixing ratios of  
484 about 10 ppbv were found during June above a *Q. pubescens* forest near Marseille (France) by  
485 Simon et al. (2005). A decrease in isoprene concentration was observed in the evening, as a  
486 consequence of isoprene emission dropping and the simultaneous consumption by OH radicals  
487 and diffusion. Isoprene mixing ratios continued to drop gradually during night time and reached  
488 their minimum in the early morning.

489 The amplitude of the isoprene air concentration diurnal cycle varied strongly from day-to-day  
490 in response to environmental condition changes. By combining all the daytime isoprene data  
491 above the canopy, a stronger correlation was found with ambient temperature than with PAR.  
492 This relationship between daytime isoprene mixing ratios and temperature (at 10 m a.g.l) was  
493 found exponential and the log linear fit of isoprene against temperature (°C) gave a relationship  
494 of  $e^{0.1334 T}$  with a coefficient of determination,  $R^2$ , of 0.79. An exponential relationship was also  
495 found between isoprene mixing ratios and temperature measured at 2 m a.g.l (Fig. 4).

496 Throughout the measurement period a clear gradient in the vertical profile of isoprene  
497 concentrations was observable, with an average of 40% higher concentrations at 2 m than at 10  
498 m a.g.l.



499 Isoprene fluxes measured during the campaign are shown in Fig. 5, along with PAR and  $u_*$   
500 measured simultaneously at 10 m. Between 10:00–17:00, PAR ranged between 200 and  
501 2015  $\mu\text{mol m}^{-2} \text{s}^{-1}$  with an average of 1500  $\mu\text{mol quanta m}^{-2} \text{s}^{-1}$ . Among the measured  
502 compounds, isoprene showed by far the largest flux values with an average daytime emission  
503 of 2.77  $\text{mg m}^{-2} \text{h}^{-1}$ . Significant positive isoprene fluxes were only observed during daytime,  
504 following diel cycles with mid-day maxima ranging from 2.0 to 9.7  $\text{mg m}^{-2} \text{h}^{-1}$ . Isoprene fluxes  
505 reached zero after sunset or were rejected due to stratified conditions ( $u_* < 0.15 \text{ m s}^{-1}$ ).

### 506 **3.2.2 MVK + MACR mixing ratios and above canopy fluxes**

507 The sum of MVK and MACR (signal at  $m/z$  71) had an average mixing ratio of 0.2 ppbv. Most  
508 of the days, MVK+MACR displayed a diurnal variability with daytime maxima ranging  
509 between 0.1 and 0.8 ppbv and nighttime minima in the order of 20-40 pptv (Fig. 6). On the 6<sup>th</sup>,  
510 15<sup>th</sup> and 16<sup>th</sup> of June, MVK+MACR did not exhibit the same diurnal trend as usually observed  
511 and its nighttime concentration remained unusually high at 0.2-0.3 ppbv. These three nights  
512 (from 5<sup>th</sup>-6<sup>th</sup>, 14<sup>th</sup>-15<sup>th</sup> and 15<sup>th</sup>-16<sup>th</sup> June) were characterized by low winds and thermally  
513 stratified conditions: indeed, the temperature profiles inside the forest canopy exhibited a clear  
514 vertical gradient (of 4 °C in 5 m) with cooler temperatures close to the forest floor.  
515 MVK+MACR high concentrations can therefore be explained by weak vertical exchanges  
516 leading to their accumulation within and just above the canopy. This suggests that night-time  
517 removal was less efficient than the high deposition rates that have recently been reported for  
518 MVK/MACR (Karl et al., 2010; Misztal et al., 2011).

519 The present study showed a strong correlation ( $R^2 = 0.84$ , slope = 0.12) between MVK+MACR  
520 and isoprene during daytime hours (07:00 am- 07:00 p.m), supporting that isoprene oxidation  
521 was responsible for the formation of the first-order oxidation products MVK and MACR. A  
522 delay of about 2 hours in the morning rise of concentrations was observed and likely represents  
523 the time that isoprene needed to be degraded.

524 Fluxes of MVK+MACR showed a general trend of emission with diurnal cycles but are  
525 subject to considerable uncertainties (Fig. 5). Indeed as MVK+MACR fluxes were small the  
526 covariance function was noisy and the true peak in the covariance function was not easily  
527 identified and consequently half of the fluxes were below the detection limit (Table 3).  
528 Considering only positive values, fluxes never exceeded 0.10  $\text{mg m}^{-2} \text{h}^{-1}$  and exhibited a mean  
529 value around 0.03  $\text{mg m}^{-2} \text{h}^{-1}$ , which equates to 3% of the isoprene flux averaged over the

530 same data points. Overall, MVK+MACR fluxes were weak and no reliable evidence of  
531 deposition was found.

### 532 **3.2.3 Monoterpenes Mixing Ratios**

533 Due to the inability of the PTR-MS to distinguish isomer molecules, only the sum of all  
534 monoterpenes was measured. Overall, the vegetation at the O<sub>3</sub>HP was a weak monoterpene  
535 emitter. Ambient concentrations derived from *m/z* 137 were low, with an average value of  
536 0.06 ppbv and a maximum at 0.25 ppbv over the whole measurement period (Fig. 3). Whereas  
537 diurnal branch-level emission rates of monoterpenes were observed for oaks and maple trees  
538 (Genard et al., 2014), ambient concentrations at the canopy level did not exhibit a clear  
539 diurnal variability. At nights, especially when the turbulence was low, a build-up of  
540 monoterpenes was observed. Night-time concentrations were probably affected by remaining  
541 emissions from the day, which were mixed over a small volume due to a shallow nocturnal  
542 boundary layer. Concentrations of monoterpenes might also be affected by advection of  
543 emissions from surrounding vegetation such as lavender or garrigue plants which are known  
544 to be monoterpenes emitters (Owen et al., 2001; Boeckelmann, 2008).

### 545 **3.2.4 Oxygenated VOC Mixing Ratios and Fluxes**

546 At the O<sub>3</sub>HP, several OxVOCs were detected. Due to their relatively long lifetimes (see Table  
547 1) and widespread sources, OxVOCs showed elevated concentrations and less pronounced  
548 diurnal cycles than isoprene. Methanol was the most abundant VOC accounting for ~40% of  
549 the total measured VOC concentrations. Methanol mixing ratios at O<sub>3</sub>HP ranged between 0.7 to  
550 5.5 ppbv (Fig. 3). Methanol's relatively long atmospheric lifetime of ~10 days (Atkinson et al.,  
551 1999) resulted in elevated background concentrations (> 0.7 ppbv). However, it was the only  
552 OxVOC with a detectable net emission flux suggesting local biogenic emissions also influence  
553 the observed concentrations. Methanol fluxes exhibited diurnal cycles with emission fluxes  
554 starting at sunrise, increasing during daytime as temperature and PAR increased, and stopping  
555 after sunset. Daily maximum methanol fluxes ranged between 0.20 and 0.63 mg m<sup>-2</sup> h<sup>-1</sup>, i.e.  
556 about 5 to 20 times lower than the isoprene fluxes. Previous studies have shown both positive  
557 and negative fluxes of methanol. In comparison, a net emission (up to 0.5 mg m<sup>-2</sup> h<sup>-1</sup>) with few  
558 transient deposition events has been reported for a tropical rainforest in Costa Rica (Karl et al.,  
559 2004), whereas a net deposition for methanol has been reported in a south-east Asian rainforest  
560 (Langford et al., 2010; Misztal et al., 2011). Our findings at the O<sub>3</sub>HP indicated that the net

561 exchange in methanol was positive. As above-canopy fluxes reflect the sum of production and  
562 removal processes, this does not mean that there was no bidirectional exchange, but that the  
563 component fluxes showing emission always overwhelmed the deposition components.

564 Among the other OxVOCs detected were acetaldehyde ( $m/z$  45), acetone ( $m/z$  59) but also three  
565 compounds with a  $m/z$  ratio of 61, 73 and 75, derived from the hourly 5 min scan. After  
566 methanol, acetone was the most abundant OxVOC with atmospheric mixing ratios ranging  
567 between 0.6 and 2.5 ppbv. Acetaldehyde followed with slightly lower concentrations around  
568 0.2-1.2 ppbv. It is striking that all of these OxVOCs mentioned above, had a good covariance  
569 (Fig. 3) and most of them correlated well with each other. The strongest correlations were  
570 between  $m/z$  45 and  $m/z$  59 ( $R^2 = 0.7$ , slope = 0.78),  $m/z$  75 and  $m/z$  61 ( $R^2 = 0.70$ )  $m/z$  59 and  
571  $m/z$  61 ( $R^2 = 0.75$ , slope = 1.2) but also  $m/z$  59 and  $m/z$  73 ( $R^2 = 0.65$ ). Correlations with  
572 methanol were lower ( $R^2 < 0.5$ ), likely due to its relatively strong biogenic source and also its  
573 high background. These significant correlations between every OxVOCs could be the result of  
574 the boundary layer dynamics, but still suggest that they had a common source or that their  
575 formation mechanisms responded to environmental factors in a similar manner. For example,  
576 the good correlation between  $m/z$  75 and  $m/z$  61, suggests that these masses include important  
577 contributions from hydroxyacetone and glycoaldehyde, two second-generation products from  
578 isoprene. However, additional contributions from other compounds cannot be excluded.

579 From the 5<sup>th</sup> to the 7<sup>th</sup> of June, changes in the wind direction were observed with air masses  
580 coming from the south and through the region of Marseille and Manosque. This southern wind  
581 shift was concurrent with the simultaneous increase of methanol, acetone, acetic acid and  
582 acetaldehyde. Respectively, from the 10<sup>th</sup> to the 14<sup>th</sup> June, when the site was under the  
583 influence of northern winds, OxVOCs were at their background levels. As OxVOCs have a  
584 relatively high lifetime of about a week, long distance transport seems to influence their  
585 ambient concentrations at the O<sub>3</sub>HP. On the other hand, the progressive and simultaneous  
586 increase of concentrations for all these OxVOCs during the last days of the field campaign (i.e  
587 14<sup>th</sup>-17<sup>th</sup> June) was remarkable, and was characterized by a steady rise in the ambient  
588 concentrations and solar radiation. This simultaneous increase of OxVOC concentration with  
589 temperature and PAR, likely reflects an additional biogenic source. Evidence of primary  
590 emission of OxVOCs has been reported for branch-level measurements from *Q. pubescens*  
591 individuals at the O<sub>3</sub>HP (Genard et al. 2014). As background levels of acetone and  
592 acetaldehyde were high and emission rates at the branch-level were very low (mean: 0.21 and

593 0.09  $\mu\text{g C g}_{\text{dry weight of biomass}}^{-1} \text{h}^{-1}$  respectively), no significant fluxes were measured above the  
594 canopy by the DEC method.

595

## 596 **4 Discussion on isoprene fluxes and in-canopy oxidation**

### 597 **4.1 Isoprene standardised flux and Biomass emission factor**

598 Isoprene fluxes presented in Section 3.2.1 confirm that emissions at the O<sub>3</sub>HP are dominated by  
599 large isoprene fluxes. During the CANOPEE field campaign, the daily maximums of the  
600 isoprene fluxes ranged between 2.0 to 9.7  $\text{mg m}^{-2} \text{h}^{-1}$  with a mean daytime flux of 2.0  $\text{mg m}^{-2} \text{h}^{-1}$ .  
601 This is in fairly good agreement with Baghi et al. (2012) who reported isoprene fluxes with  
602 values in the range 5.4–10  $\text{mg m}^{-2} \text{h}^{-1}$  around midday, measured by DEC during a 2-day period  
603 in early August 2010 at the same site.

604 To our knowledge, above-canopy isoprene fluxes recorded at the O<sub>3</sub>HP are the largest reported  
605 in the Mediterranean basin. Most of the VOC studies in this region were about monoterpenes  
606 emitters. In western Italy, above a low macchia ecosystem, Davison et al. (2009) reported  
607 relatively small isoprene fluxes with mean daytime values of 0.097; 0.016 and 0.032  $\text{mg m}^{-2} \text{h}^{-1}$   
608 measured using the DEC method with three different PTR-MS. Furthermore, no significant  
609 isoprene fluxes were found above a pine-oak forest site in Italy and above orange plantations in  
610 Spain during the BEMA's field studies (Velentini et al., 1997; Darmais et al., 2000). As the  
611 number of isoprene flux measurements at the canopy level in the Mediterranean region is  
612 limited, we extend our comparison to other ecosystems in the world. A non-exhaustive  
613 overview of isoprene flux measurements in Mediterranean, tropical, and temperate ecosystems  
614 is presented in Table 4. Reported values are displayed as found in the reference papers and  
615 demonstrate a difficulty of intercomparison due to the multiple statistical ways of expressing  
616 the results (mean, median, range) used in every study. However, this table gives an idea of the  
617 orders of magnitude of isoprene emission rates at the canopy scale, and confirms that isoprene  
618 emissions from Mediterranean forests can be similar to or higher than those observed in other  
619 regions of the world which are dominated by isoprene-emitting vegetation. For instance,  
620 maximum isoprene fluxes of 6.1, 7.1, and 10.8  $\text{mg m}^{-2} \text{h}^{-1}$  were observed respectively above a  
621 mature lowland in the Central Amazon (Kuhn et al., 2007), a coniferous forest in eastern  
622 Belgium (Laffineur et al., 2011) or a deciduous forest in Germany (Spirig et al., 2005) and are  
623 very close to the maxima recorded at the O<sub>3</sub>HP. Considerably higher isoprene fluxes reaching

624 up to  $30 \text{ mg m}^{-2} \text{ h}^{-1}$  were reported only from an oil palm plantation in Malaysia (Miształ et al.,  
625 2011)

626 Isoprene fluxes at the O<sub>3</sub>HP were also normalized to standard conditions (temperature and PAR  
627 at the canopy level of  $30 \text{ }^\circ\text{C}$  and  $1000 \text{ } \mu\text{mol m}^{-2} \text{ s}^{-1}$  respectively) using the G93 algorithm  
628 (Guenther et al., 1993). By plotting all measured fluxes against the combined temperature and  
629 light scaling factors ( $C_L$ ,  $C_T$ ), a standardized flux  $F_{\text{standard}}$  (or basal emission rate) of  $7.43 \text{ mg m}^{-2}$   
630  $\text{h}^{-1}$  was derived from the fit line with zero intercept (Fig. 7).

631 For comparison, enclosure measurements for 7 different branches of *Q.pubescens* at the  
632 O<sub>3</sub>HP during CANOPEE resulted in emission factors  $EF_{\text{biomass}}$  ranging between 30-140  
633  $\mu\text{g g}_{\text{dry weight of biomass}}^{-1} \text{ h}^{-1}$  (hereafter,  $\mu\text{g g}_{\text{dwt}}^{-1} \text{ h}^{-1}$ ) with a median value of  $70 \pm 8 \mu\text{g g}_{\text{dwt}}^{-1} \text{ h}^{-1}$   
634 (Genard et al., 2014). The average  $EF_{\text{biomass}}$  was then upscaled to give an standardized flux  
635  $F_{\text{standard}}$ :

$$636 \quad F_{\text{standard-upscaled}} = EF_{\text{biomass}} \times \sum_{h=0}^{h_c} LAI(h) * LMA(h) \quad (3)$$

637 where  $h$  is the distance above ground (unit: m),  $h_c$  the canopy height, LAI the mean leaf area  
638 index (unit:  $\text{m}^{-2} \cdot \text{m}^{-2}$ ) and LMA the leaf dry mass per unit area (unit:  $\text{g} \cdot \text{m}^{-2}$ ). The resulting up-  
639 scaled basal emission rate  $F_{\text{standard-upscaled}}$  was  $18 \pm 5 \text{ mg m}^{-2} \text{ h}^{-1}$ . Fluxes estimated by  
640 extrapolating leaf-level measurements were two fold higher than the average figure derived  
641 from DEC measurements. We consider this to be a reasonably good agreement since a factor  
642 of 2 of difference can be expected when comparing techniques over different spatial scales,  
643 due to uncertainties in the extrapolation, in addition to the uncertainties on both  
644 measurements. A reason for the difference certainly arises also from the normalization of  
645 DEC fluxes to standard conditions using the air temperature and PAR above the canopy.  
646 Since a significant fraction of the canopy experiences lower light levels, the standardised  
647 emission flux using an above-canopy PAR is under-estimated. For example, a normalization  
648 using an in-canopy PAR would lead to an  $F_{\text{standard}}$  increase of about 100%. On the other hand,  
649 the normalization using actual leaf temperature, which is usually a couple of degrees higher  
650 than ambient temperature, would lead to lower  $F_{\text{standard}}$  values. A canopy structure model  
651 would be required to better quantify both effects. Additional uncertainty comes from the  
652 difference in biomass emission factors  $EF_{\text{biomass}}$ , which, can vary by more than a factor of 4  
653 between tree individuals, as indicated by the branch-level measurements (Genard et al., 2014).  
654 Leaf level measurements are often performed on sun foliage, which has larger emission rates  
655 as compared to the whole crown. Further, an overestimation of basal emission rates based on

656 leaf level emissions could be the chemical loss of isoprene within the canopy, which we  
657 tentatively examine hereafter.

## 658 **4.2 Isoprene oxidation within the canopy**

659 In recent years, more attention has been put to understand isoprene chemistry, particularly in  
660 sites such as the O<sub>3</sub>HP, where the isoprene emissions are strong and the NO<sub>x</sub> levels are low  
661 (NO mean value ~25 ppt). Inconsistencies between observations in rural sites and model  
662 estimates of the ratio of isoprene to its oxidation products have pointed out uncertainties  
663 associated with the understanding of the mechanism of isoprene oxidation. Lately, laboratory  
664 studies have elaborated rate coefficients and product branching ratios yields (Paulot et al.,  
665 2009; Peeters et al., 2009; Silva et al., 2009; Peeters and Müller, 2010; Fuchs et al., 2013). In  
666 the following section, we investigate the isoprene oxidation and production of MVK and  
667 MACR at the O<sub>3</sub>HP and discuss our results with regard to recent findings that suggest very  
668 low production yields of MVK and MACR under low NO<sub>x</sub> conditions (NO<70ppt) (Liu et al.,  
669 2013).

670 OH-oxidation of isoprene is initiated by the addition of the hydroxy radical to the double  
671 bonds of isoprene. The alkyl radical formed reacts with oxygen (O<sub>2</sub>) to form alkyl peroxy  
672 radicals (HO<sub>2</sub>C<sub>5</sub>H<sub>8</sub>O<sub>2</sub>°), commonly called ISOPOO. ISOPOO radicals subsequently react  
673 either with NO (Tuazon and Atkinson 1990), hydroperoxy radicals HO<sub>2</sub> (Paulot et al.,  
674 2009), or organic peroxy radicals RO<sub>2</sub> (Jenkin et al. 1998). Additional isomerization  
675 reactions of ISOPOO radicals have also been suggested in the recent literature (Peeters et al.  
676 2009, da Silva et al.; 2010, Fuchs et al., 2013). At high NO<sub>x</sub> concentrations the dominant fate  
677 of ISOPOO is generally the reaction with NO. However, under low NO<sub>x</sub> conditions, reaction  
678 with HO<sub>2</sub> dominates and leads to lower MVK and MACR yields (Miyoshi et al. 1994, Ruper  
679 and Becker 2000). Using atmospheric simulation chambers, Liu et al. (2013) found the lowest  
680 MVK and MACR yields that have ever been reported, with values of (3.8±1.3)% for MVK  
681 and (2.5±0.9)% for MACR, i.e. more than 60% less than in previous “low-NO<sub>x</sub>” studies  
682 (Miyoshi et al. 1994, Ruper and Becker 2000, Navarro et al., 2011), and about 10 times lower  
683 than via the NO pathway.

684 At the O<sub>3</sub>HP, the twelve days of measurements featured a [MVK+MACR]-to-isoprene ratio  
685 of 0.13±0.05 during daytime (Fig. 8). It has to be considered that this ratio could be lower if  
686 any interference occurred at *m/z* 71 from other oxidation products. Despite this possible  
687 overestimation, the [MVK+MACR]-to-isoprene ratio at the O<sub>3</sub>HP is at the lower end of the

688 range that has previously been observed in other ecosystems of the world, and could be  
689 explained by the very low NO<sub>x</sub> conditions. This ratio usually fall around 0.3-0.75, and is also  
690 dependent on the sampling height (Montzka et al., 1993; Biesenthal et al., 1998; Holzinger et  
691 al., 2002). Nevertheless, a few studies have shown ratios close to our estimates: a ratio of 0.12  
692 has been reported in a rural forest of Michigan (Apel, 2002), and a ratio of 0.1 to 0.36 was  
693 obtained in a South-East Asian tropical rainforest (Langford et al., 2010).

694 Fluxes of mass 71 (related to MACR and MVK and possible contribution from isoprene  
695 hydroperoxides), showed a general trend of emission and thus, suggest a production  
696 throughout the forest canopy. However, the magnitude of these fluxes was very low: about  
697 40% being below the detection limit, and the data that passed all the quality assessment tests  
698 represented about 3% of the isoprene fluxes. Estimates of the isoprene that is oxidated to  
699 MVK+MACR below the sampling height of flux measurement are usually in order of 5 to  
700 15%, also depending on the measurement height (Stroud et al., 2005). Additionally to the low  
701 NO<sub>x</sub> conditions, which lead to low yields of MACR and MVK, minor chemical processing of  
702 isoprene is expected below the measurement height due to the canopy architecture of the  
703 O<sub>3</sub>HP. The forest of the O<sub>3</sub>HP is low (5 m height on average), well ventilated and therefore  
704 closely coupled to the boundary layer above. Thus, the turbulent transport time  $\tau$  between  
705 ground surface and the measurement height was estimated to be around 30-60 s in daytime  
706 (See Supplementary Material for calculation details). This is considerably faster than the  
707 isoprene chemical degradation estimated at about 4 hours against its oxidation by OH for  
708 typical summer daytime. Thus, isoprene rapidly reaches the atmosphere and does not have the  
709 time to react in a significant way with OH radicals from the moment of its release by the  
710 vegetation and its arrival at the sampling inlet.

711

## 712 **Conclusions**

713 We have presented atmospheric measurements at high resolution for concentrations and direct  
714 above-canopy fluxes of BVOCs for a Mediterranean downy oak forest.

715 High concentrations of isoprene have been observed, with daytime maxima ranging between  
716 2-17 ppbv inside the forest and 2-5 ppbv above the top of the canopy. Isoprene concentrations  
717 showed a clear diurnal cycle with a daytime maximum and a minimum in the early morning  
718 and at night, respectively. Above the canopy, isoprene concentrations were about 40% lower  
719 than inside the canopy; this loss was attributed to physical processes such as mixing with  
720 isoprene-depleted air masses (or, conversely, the build-up of isoprene within the canopy).

721 Isoprene fluxes at the O<sub>3</sub>HP site were among the largest fluxes reported in the Mediterranean  
722 region, with mid-day maxima ranging between 2.0-9.7 mg m<sup>-2</sup> h<sup>-1</sup>. Based on these  
723 measurements, an isoprene basal emission rate of 7.43 mg m<sup>-2</sup> h<sup>-1</sup> is recommended for downy  
724 oaks in this region for biogenic emission models. OxVOCs were abundant at the site with  
725 mean daytime concentration of 2.48, 1.35 and 0.42 ppbv for methanol, acetone and  
726 acetaldehyde respectively. Of these compounds, only methanol exhibited significant fluxes,  
727 indicating a primary source inside the canopy. Methanol fluxes featured maxima daytime  
728 values ranging between 0.20-0.63 mg m<sup>-2</sup> h<sup>-1</sup>, i.e about 5 to 20 times lower than isoprene  
729 fluxes. No above-canopy fluxes of monoterpenes have been observed, and, as a result,  
730 ambient concentrations of monoterpenes were close to the detection limits. These  
731 observations are in agreement with a branch-level study, stating that *Q.pubescens* was a  
732 strong emitter of isoprene and weak emitter of monoterpenes (Genard et al. 2014).

733 At the forest site of the O<sub>3</sub>HP, where the isoprene emissions were high and the NO<sub>x</sub> levels  
734 low, a small [MVK+MACR]-to-isoprene ratio has been observed (mean daytime value of  
735 0.13±0.05). Up-ward fluxes of MACR and MVK indicated a production from isoprene  
736 throughout the forest canopy, but represented less than 3% of the isoprene flux. Further, no  
737 systematic deposition fluxes could be detected for either of the investigated compounds.  
738 Therefore, we conclude that intra-canopy processes had a minor effect on above-canopy  
739 fluxes.

740

## 741 **Acknowledgements**

742 We thank our colleagues for continuous support and discussion. We are grateful to the O<sub>3</sub>HP  
743 team and especially to J.P. Orts and T. Gauquelin. We thank A. Bouygues for helping with the  
744 setup. This work is supported by the French National Agency for Research (ANR 2010 JCJC  
745 603 01). We acknowledge the INSU (ChARMEx), ADEME, CNRS and CEA for supporting  
746 funding. The CEH contribution to the study was supported by the FP7 project ÉCLAIRE.

747



748 **References**

- 749 Andreae, M. O. and Crutzen, P. J.: Atmospheric Aerosols: Biogeochemical Sources and Role  
750 in Atmospheric Chemistry, Science, 276(5315), 1052–1058,  
751 doi:10.1126/science.276.5315.1052, 1997.
- 752 Apel, E. C.: Measurement and interpretation of isoprene fluxes and isoprene, methacrolein,  
753 and methyl vinyl ketone mixing ratios at the PROPHET site during the 1998 Intensive,  
754 Journal of Geophysical Research, 107(D3), doi:10.1029/2000JD000225, 2002.
- 755 Atkinson, R., Baulch, D. L., Cox, R. A., Hampson, R. F., Kerr, J. A., Rossi, M. J. and Troe,  
756 J.: Evaluated Kinetic and Photochemical Data for Atmospheric Chemistry, Organic Species:  
757 Supplement VII, Journal of Physical and Chemical Reference Data, 28(2), 191,  
758 doi:doi:10.1063/1.556048, 1999.
- 759 Baghi, R., Durand, P., Jambert, C., Jarnot, C., Delon, C., Serça, D., Striebig, N., Ferlicoq, M.  
760 and Keravec, P.: A new disjunct eddy-covariance system for BVOC flux measurements  
761 &ndash; validation on CO<sub>2</sub> and H<sub>2</sub>O fluxes, Atmospheric Measurement Techniques, 5(12),  
762 3119–3132, doi:10.5194/amt-5-3119-2012, 2012.
- 763 Biesenthal, T. A., Bottenheim, J. W., Shepson, P. B., Li, S.-M. and Brickell, P. C.: The  
764 chemistry of biogenic hydrocarbons at a rural site in eastern Canada, Journal of Geophysical  
765 Research: Atmospheres, 103(D19), 25487–25498, doi:10.1029/98JD01848, 1998.
- 766 Blake, R. S., Monks, P. S. and Ellis, A. M.: Proton-Transfer Reaction Mass Spectrometry,  
767 Chemical Reviews, 109(3), 861–896, doi:10.1021/cr800364q, 2009.
- 768 Boeckelmann, A.: Monoterpene production and regulation in lavenders (*Lavandula*  
769 *angustifolia* and *Lavandula x intermedia*), [online] Available from:  
770 <https://circle.ubc.ca/handle/2429/2804> (Accessed 27 September 2013), 2008.
- 771 Chameides, W. L., Lindsay, R. W., Richardson, J. and Kiang, C. S.: The role of biogenic  
772 hydrocarbons in urban photochemical smog: Atlanta as a case study, Science, 241(4872),  
773 1473–1475, doi:10.1126/science.3420404, 1988.
- 774 Chiemchaisri, W., Visvanathan, C. and Jy, S. W.: Effects of trace volatile organic compounds  
775 on methane oxidation, Brazilian Archives of Biology and Technology, 44(2), 135–140,  
776 doi:10.1590/S1516-89132001000200005, 2001.
- 777 Christian, T. J., Kleiss, B., Yokelson, R. J., Holzinger, R., Crutzen, P. J., Hao, W. M., Shirai,  
778 T. and Blake, D. R.: Comprehensive laboratory measurements of biomass-burning emissions:  
779 2. First intercomparison of open-path FTIR, PTR-MS, and GC-MS/FID/ECD, Journal of  
780 Geophysical Research: Atmospheres, 109(D2), n/a–n/a, doi:10.1029/2003JD003874, 2004.
- 781 Ciccioli, P., Brancaleoni, E., Frattoni, M., Di Palo, V., Valentini, R., Tirone, G., Seufert, G.,  
782 Bertin, N., Hansen, U., Csiky, O., Lenz, R. and Sharma, M.: Emission of reactive terpene  
783 compounds from orange orchards and their removal by within-canopy processes, Journal of  
784 Geophysical Research: Atmospheres, 104(D7), 8077–8094, doi:10.1029/1998JD100026,  
785 1999.

- 786 Claeys, M., Graham, B., Vas, G., Wang, W., Vermeylen, R., Pashynska, V., Cafmeyer, J.,  
787 Guyon, P., Andreae, M. O., Artaxo, P. and Maenhaut, W.: Formation of Secondary Organic  
788 Aerosols Through Photooxidation of Isoprene, *Science*, 303(5661), 1173–1176,  
789 doi:10.1126/science.1092805, 2004.
- 790 Clarke, J. U.: Evaluation of censored data methods to allow statistical comparisons among  
791 very small samples with below detection limit observations, *Environmental science &*  
792 *technology*, 32(1), 177–183, 1998.
- 793 Curci, G., Palmer, P. I., Kurosu, T. P., Chance, K. and Visconti, G.: Estimating European  
794 volatile organic compound emissions using satellite observations of formaldehyde from the  
795 Ozone Monitoring Instrument, *Atmos. Chem. Phys.*, 10(23), 11501–11517, doi:10.5194/acp-  
796 10-11501-2010, 2010.
- 797 Darmais, S., Dutaur, L., Larsen, B., Cieslik, S., Luchetta, L., Simon, V. and Torres, L.:  
798 Emission fluxes of VOC by orange trees determined by both relaxed eddy accumulation and  
799 vertical gradient approaches, *Chemosphere - Global Change Science*, 2(1), 47–56,  
800 doi:10.1016/S1465-9972(99)00050-1, 2000.
- 801 Davison, B., Taipale, R., Langford, B., Miształ, P., Fares, S., Matteucci, G., Loreto, F., Cape,  
802 J. N., Rinne, J. and Hewitt, C. N.: Concentrations and fluxes of biogenic volatile organic  
803 compounds above a Mediterranean macchia ecosystem in western Italy, *Biogeosciences*, 6(8),  
804 1655–1670, doi:10.5194/bg-6-1655-2009, 2009a.
- 805 Davison, B., Taipale, R., Langford, B., Miształ, P., Fares, S., Matteucci, G., Loreto, F., Cape,  
806 J. N., Rinne, J. and Hewitt, C. N.: Concentrations and fluxes of biogenic volatile organic  
807 compounds above a Mediterranean macchia ecosystem in western Italy, *Biogeosciences*, 6(8),  
808 1655–1670, doi:10.5194/bg-6-1655-2009, 2009b.
- 809 Forkel, R., Klemm, O., Graus, M., Rappenglück, B., Stockwell, W. R., Grabmer, W., Held,  
810 A., Hansel, A. and Steinbrecher, R.: Trace gas exchange and gas phase chemistry in a Norway  
811 spruce forest: A study with a coupled 1-dimensional canopy atmospheric chemistry emission  
812 model, *Atmospheric Environment*, 40, Supplement 1, 28–42,  
813 doi:10.1016/j.atmosenv.2005.11.070, 2006.
- 814 Fuchs, H., Hofzumahaus, A., Rohrer, F., Bohn, B., Brauers, T., Dorn, H. P., Häsel, R.,  
815 Holland, F., Kaminski, M. and Li, X.: Experimental evidence for efficient hydroxyl radical  
816 regeneration in isoprene oxidation, *Nature Geoscience* [online] Available from:  
817 <http://www.nature.com/ngeo/journal/vaop/ncurrent/full/ngeo1964.html> (Accessed 21 May  
818 2014), 2013.
- 819 Fuentes, J. D., Lerdau, M., Atkinson, R., Baldocchi, D., Bottenheim, J. W., Ciccioli, P.,  
820 Lamb, B., Geron, C., Gu, L., Guenther, A. and others: Biogenic hydrocarbons in the  
821 atmospheric boundary layer: a review, *BULLETIN-AMERICAN METEOROLOGICAL*  
822 *SOCIETY*, 81(7), 1537–1576, 2000.
- 823 Genard, A.-C., Boissard, C., Ormeno, E., Kalogridis, C., Fernandez, C., Gros, V., Lathière,  
824 J., Orts, J.-P., Bonnaire, N. and Ormeno, E.: Variability of BVOC emissions from a  
825 Mediterranean mixed forest with focus on *Quercus pubescens* at the O3HP,, to be submitted.

- 826 Goldstein, A. H. and Galbally, I. E.: Known and unexplored organic constituents in the  
827 earth's atmosphere, *Environmental Science & Technology*, 41(5), 1514–1521, 2007.
- 828 Goldstein, A. H., Goulden, M. L., Munger, J. W., Wofsy, S. C. and Geron, C. D.: Seasonal  
829 course of isoprene emissions from a midlatitude deciduous forest, *Journal of Geophysical*  
830 *Research: Atmospheres*, 103(D23), 31045–31056, doi:10.1029/98JD02708, 1998.
- 831 De Gouw, J. and Warneke, C.: Measurements of volatile organic compounds in the earth's  
832 atmosphere using proton-transfer-reaction mass spectrometry, *Mass Spectrometry Reviews*,  
833 26(2), 223–257, 2006.
- 834 De Gouw, J. and Warneke, C.: Measurements of volatile organic compounds in the earth's  
835 atmosphere using proton-transfer-reaction mass spectrometry, *Mass Spectrometry Reviews*,  
836 26(2), 223–257, 2007.
- 837 Griffin, R. J., Cocker, D. R., Flagan, R. C. and Seinfeld, J. H.: Organic aerosol formation  
838 from the oxidation of biogenic hydrocarbons, *Journal of Geophysical Research: Atmospheres*,  
839 104(D3), 3555–3567, doi:10.1029/1998JD100049, 1999.
- 840 Guenther, A. B., Jiang, X., Heald, C. L., Sakulyanontvittaya, T., Duhl, T., Emmons, L. K. and  
841 Wang, X.: The Model of Emissions of Gases and Aerosols from Nature version 2.1  
842 (MEGAN2.1): an extended and updated framework for modeling biogenic emissions,  
843 *Geoscientific Model Development*, 5(6), 1471–1492, doi:10.5194/gmd-5-1471-2012, 2012.
- 844 Guenther, A. B., Zimmerman, P. R., Harley, P. C., Monson, R. K. and Fall, R.: Isoprene and  
845 monoterpene emission rate variability: Model evaluations and sensitivity analyses, *Journal of*  
846 *Geophysical Research: Atmospheres*, 98(D7), 12609–12617, doi:10.1029/93JD00527, 1993.
- 847 Guenther, A., Hewitt, C. N., Erickson, D., Fall, R., Geron, C., Graedel, T., Harley, P.,  
848 Klinger, L., Lerdau, M., McKay, W. A., Pierce, T., Scholes, B., Steinbrecher, R., Tallamraju,  
849 R., Taylor, J. and Zimmerman, P.: A global model of natural volatile organic compound  
850 emissions, *Journal of Geophysical Research: Atmospheres*, 100(D5), 8873–8892,  
851 doi:10.1029/94JD02950, 1995.
- 852 Haase, K. B., Keene, W. C., Pszenny, A. A. P., Mayne, H. R., Talbot, R. W. and Sive, B. C.:  
853 Calibration and intercomparison of acetic acid measurements using proton-transfer-reaction  
854 mass spectrometry (PTR-MS), *Atmos. Meas. Tech.*, 5(11), 2739–2750, doi:10.5194/amt-5-  
855 2739-2012, 2012.
- 856 Helsel, D. R. and Hirsch, R. M.: *Statistical methods in water resources*, Elsevier. [online]  
857 Available from:  
858 [http://books.google.fr/books?hl=fr&lr=&id=jao4o5X1pvgC&oi=fnd&pg=PP2&dq=Helsel+an](http://books.google.fr/books?hl=fr&lr=&id=jao4o5X1pvgC&oi=fnd&pg=PP2&dq=Helsel+and+Hirsch,+1992&ots=QUPzeLd4J_&sig=8nnOroZFKIJvnN_wgKf3slP7tCQ)  
859 [d+Hirsch,+1992&ots=QUPzeLd4J\\_&sig=8nnOroZFKIJvnN\\_wgKf3slP7tCQ](http://books.google.fr/books?hl=fr&lr=&id=jao4o5X1pvgC&oi=fnd&pg=PP2&dq=Helsel+and+Hirsch,+1992&ots=QUPzeLd4J_&sig=8nnOroZFKIJvnN_wgKf3slP7tCQ) (Accessed 21  
860 May 2014), 1992.
- 861 Hodzic, A., Madronich, S., Aumont, B., Lee-Taylor, J., Karl, T., Camredon, M. and Mouchel-  
862 Vallon, C.: Limited influence of dry deposition of semivolatile organic vapors on secondary  
863 organic aerosol formation in the urban plume, *Geophys. Res. Lett.*, 40(12), 3302–3307,  
864 doi:10.1002/grl.50611, 2013.

- 865 Holzinger, R., Sanhueza, E., Von Kuhlmann, R., Kleiss, B., Donoso, L. and Crutzen, P. J.:  
866 Diurnal cycles and seasonal variation of isoprene and its oxidation products in the tropical  
867 savanna atmosphere, *Global Biogeochemical Cycles*, 16(4), 22–1–22–13,  
868 doi:10.1029/2001GB001421, 2002.
- 869 Horst, T. W.: A SIMPLE FORMULA FOR ATTENUATION OF EDDY FLUXES  
870 MEASURED WITH FIRST-ORDER-RESPONSE SCALAR SENSORS, *Boundary-Layer*  
871 *Meteorology*, 82(2), 219–233, doi:10.1023/A:1000229130034, 1997.
- 872 Jacob, D. J. and Wofsy, S. C.: Photochemistry of biogenic emissions over the Amazon forest,  
873 *Journal of Geophysical Research: Atmospheres*, 93(D2), 1477–1486,  
874 doi:10.1029/JD093iD02p01477, 1988.
- 875 Karl, T. G., Spirig, C., Rinne, J., Stroud, C., Prevost, P., Greenberg, J., Fall, R. and Guenther,  
876 A.: Virtual disjunct eddy covariance measurements of organic compound fluxes from a  
877 subalpine forest using proton transfer reaction mass spectrometry, *Atmospheric Chemistry*  
878 *and Physics*, 2(4), 279–291, doi:10.5194/acpd-2-999-2002, 2002.
- 879 Karl, T., Guenther, A., Turnipseed, A., Tyndall, G., Artaxo, P. and Martin, S.: Rapid  
880 formation of isoprene photo-oxidation products observed in Amazonia, *Atmospheric*  
881 *Chemistry and Physics*, 9(20), 7753–7767, 2009.
- 882 Karl, T., Guenther, A., Yokelson, R. J., Greenberg, J., Potosnak, M., Blake, D. R. and Artaxo,  
883 P.: The tropical forest and fire emissions experiment: Emission, chemistry, and transport of  
884 biogenic volatile organic compounds in the lower atmosphere over Amazonia, *Journal of*  
885 *Geophysical Research*, 112(D18), doi:10.1029/2007JD008539, 2007.
- 886 Karl, T., Harley, P., Emmons, L., Thornton, B., Guenther, A., Basu, C., Turnipseed, A. and  
887 Jardine, K.: Efficient Atmospheric Cleansing of Oxidized Organic Trace Gases by  
888 Vegetation, *Science*, 330(6005), 816–819, doi:10.1126/science.1192534, 2010.
- 889 Karl, T., Potosnak, M., Guenther, A., Clark, D., Walker, J., Herrick, J. D. and Geron, C.:  
890 Exchange processes of volatile organic compounds above a tropical rain forest: Implications  
891 for modeling tropospheric chemistry above dense vegetation, *J. Geophys. Res.*, 109(D18),  
892 D18306, doi:10.1029/2004JD004738, 2004.
- 893 Keenan, T., Niinemets, Ü., Sabate, S., Gracia, C. and Penuelas, J.: Process based inventory of  
894 isoprenoid emissions from European forests: model comparisons, current knowledge and  
895 uncertainties, *Atmospheric Chemistry and Physics*, 9(12), 4053–4076, 2009.
- 896 Kesselmeier, J., Bode, K., Schäfer, L., Schebeske, G., Wolf, A., Brancaleoni, E., Cecinato, A.,  
897 Ciccioli, P., Frattoni, M., Dutaur, L., Fugit, J. L., Simon, V. and Torres, L.: Simultaneous  
898 field measurements of terpene and isoprene emissions from two dominant mediterranean oak  
899 species in relation to a North American species, *Atmospheric Environment*, 32(11), 1947–  
900 1953, doi:10.1016/S1352-2310(97)00500-1, 1998.
- 901 Kesselmeier J. and Staudt M.: Biogenic Volatile Organic Compounds (VOC): An Overview  
902 on Emission, Physiology and Ecology, *Journal of Atmospheric Chemistry*, 33(1), 23–88

- 903 Kljun, N., Calanca, P., Rotach, M. W. and Schmid, H. P.: A Simple Parameterisation for Flux  
904 Footprint Predictions, *Boundary-Layer Meteorology*, 112(3), 503–523,  
905 doi:10.1023/B:BOUN.0000030653.71031.96, 2004.
- 906 Kuhn, U., Andreae, M. O., Ammann, C., Araujo, A. C., Brancaleoni, E., Ciccioli, P., Dindorf,  
907 T., Frattoni, M., Gatti, L. V., Ganzeveld, L., Kruijt, B., Lelieveld, J., Lloyd, J., Meixner, F.  
908 X., Nobre, A. D., Poeschl, U., Spirig, C., Stefani, P., Thielmann, A., Valentini, R. and  
909 Kesselmeier, J.: Isoprene and monoterpene fluxes from Central Amazonian rainforest inferred  
910 from tower-based and airborne measurements, and implications on the atmospheric chemistry  
911 and the local carbon budget, *Atmos. Chem. Phys.*, 7(11), 2855–2879, 2007.
- 912 Laffineur, Q., Aubinet, M., Schoon, N., Amelynck, C., Mueller, J.-F., Dewulf, J., Van  
913 Langenhove, H., Steppe, K., Simpraga, M. and Heinesch, B.: Isoprene and monoterpene  
914 emissions from a mixed temperate forest RID F-3549-2011, *Atmos. Environ.*, 45(18), 3157–  
915 3168, doi:10.1016/j.atmosenv.2011.02.054, 2011.
- 916 Langford, B., Davison, B., Nemitz, E. and Hewitt, C. N.: Mixing ratios and eddy covariance  
917 flux measurements of volatile organic compounds from an urban canopy (Manchester, UK),  
918 *Atmos. Chem. Phys.*, 9(6), 1971–1987, doi:10.5194/acp-9-1971-2009, 2009.
- 919 Langford, B., Misztal, P. K., Nemitz, E., Davison, B., Helfter, C., Pugh, T. A. M.,  
920 MacKenzie, A. R., Lim, S. F. and Hewitt, C. N.: Fluxes and concentrations of volatile organic  
921 compounds from a South-East Asian tropical rainforest, *Atmospheric Chemistry and Physics  
922 Discussions*, 10(5), 11975–12021, doi:10.5194/acpd-10-11975-2010, 2010.
- 923 Laothawornkitkul, J., Taylor, J. E., Paul, N. D. and Hewitt, C. N.: Biogenic volatile organic  
924 compounds in the Earth system, *New Phytologist*, 183(1), 27–51, 2009.
- 925 Lee, J. D., Lewis, A. C., Monks, P. S., Jacob, M., Hamilton, J. F., Hopkins, J. R., Watson, N.,  
926 Saxton, J., Ennis, C., Carpenter, L. J., Fleming, Z. L., Bandy, B. J., Mills, G. P., Oram, D. E.,  
927 Penkett, S. A., Slemr, J., Norton, E., Vaughan, G., Rickard, A. R., Whalley, L. K., Heard, D.  
928 E., Bloss, W. J., Gravestock, T., Johnson, G., Ingham, T., Smith, S. C., Seakins, P. W., Cryer,  
929 D., Stanton, J., Pilling, M. J., McQuaid, J. B., Jenkin, M. E., Utembe, S., Johnson, D., Coe,  
930 H., Bower, K., Gallagher, M., McFiggans, G., Carslaw, N. and Emmerson, K. M.: Ozone  
931 photochemistry during the UK heat wave of August 2003, *Ozone photochemistry and  
932 elevated isoprene during the UK heatwave of August 2003* [online] Available from:  
933 <https://ira.le.ac.uk/handle/2381/307> (Accessed 21 November 2013), 2006.
- 934 Liu, Y. J., Herdlinger-Blatt, I., McKinney, K. A. and Martin, S. T.: Production of methyl  
935 vinyl ketone and methacrolein via the hydroperoxyl pathway of isoprene oxidation,  
936 *Atmospheric Chemistry and Physics*, 13(11), 5715–5730, 2013.
- 937 Makar, P. A., Fuentes, J. D., Wang, D., Staebler, R. M. and Wiebe, H. A.: Chemical  
938 processing of biogenic hydrocarbons within and above a temperate deciduous forest, *Journal  
939 of Geophysical Research: Atmospheres*, 104(D3), 3581–3603, doi:10.1029/1998JD100065,  
940 1999.
- 941 McKinney, K. A., Lee, B. H., Vasta, A., Pho, T. V. and Munger, J. W.: Emissions of  
942 isoprenoids and oxygenated biogenic volatile organic compounds from a New England  
943 mixed forest, *Atmos. Chem. Phys.*, 11(10), 4807–4831, doi:10.5194/acp-11-4807-2011, 2011.

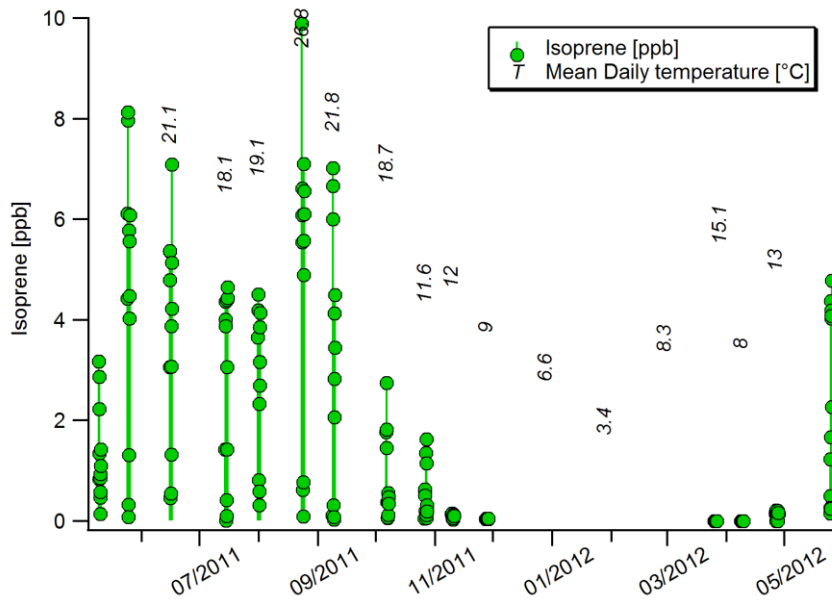
- 944 Misztal, P. K., Nemitz, E., Langford, B., Di Marco, C. F., Phillips, G. J., Hewitt, C. N.,  
945 MacKenzie, A. R., Owen, S. M., Fowler, D., Heal, M. R. and Cape, J. N.: Direct ecosystem  
946 fluxes of volatile organic compounds from oil palms in South-East Asia, *Atmospheric*  
947 *Chemistry and Physics*, 11(17), 8995–9017, doi:10.5194/acp-11-8995-2011, 2011.
- 948 Montzka, S. A., Trainer, M., Goldan, P. D., Kuster, W. C. and Fehsenfeld, F. C.: Isoprene and  
949 its oxidation products, methyl vinyl ketone and methacrolein, in the rural troposphere, *Journal*  
950 *of Geophysical Research: Atmospheres*, 98(D1), 1101–1111, doi:10.1029/92JD02382, 1993.
- 951 Owen, S. M., Boissard, C. and Hewitt, C. N.: Volatile organic compounds (VOCs) emitted  
952 from 40 Mediterranean plant species:: VOC speciation and extrapolation to habitat scale,  
953 *Atmospheric Environment*, 35(32), 5393–5409, doi:10.1016/S1352-2310(01)00302-8, 2001.
- 954 Park, J.-H., Goldstein, A. H., Timkovsky, J., Fares, S., Weber, R., Karlik, J. and Holzinger,  
955 R.: Eddy covariance emission and deposition flux measurements using proton transfer  
956 reaction – time of flight – mass spectrometry (PTR-TOF-MS): comparison with PTR-MS  
957 measured vertical gradients and fluxes, *Atmos. Chem. Phys.*, 13(3), 1439–1456,  
958 doi:10.5194/acp-13-1439-2013, 2013.
- 959 Paulot, F., Crounse, J. D., Kjaergaard, H. G., Kürten, A., Clair, J. M. S., Seinfeld, J. H. and  
960 Wennberg, P. O.: Unexpected epoxide formation in the gas-phase photooxidation of isoprene,  
961 *Science*, 325(5941), 730–733, 2009.
- 962 Peeters, J. and Müller, J.-F.: HOx radical regeneration in isoprene oxidation via peroxy  
963 radical isomerisations. II: experimental evidence and global impact, *Physical Chemistry*  
964 *Chemical Physics*, 12(42), 14227–14235, 2010.
- 965 Peeters, J., Nguyen, T. L. and Vereecken, L.: HOx radical regeneration in the oxidation of  
966 isoprene, *Physical Chemistry Chemical Physics*, 11(28), 5935–5939, 2009.
- 967 Richards, N. A. D., Arnold, S. R., Chipperfield, M. P., Miles, G., Rap, A., Siddans, R.,  
968 Monks, S. A. and Hollaway, M. J.: The Mediterranean summertime ozone maximum: global  
969 emission sensitivities and radiative impacts, *Atmos. Chem. Phys.*, 13(5), 2331–2345,  
970 doi:10.5194/acp-13-2331-2013, 2013.
- 971 Rinne, H. J. I., Guenther, A. B., Greenberg, J. P. and Harley, P. C.: Isoprene and monoterpene  
972 fluxes measured above Amazonian rainforest and their dependence on light and temperature,  
973 *Atmospheric Environment*, 36(14), 2421–2426, doi:10.1016/S1352-2310(01)00523-4, 2002.
- 974 Rinne, H. J. I., Guenther, A. B., Warneke, C., Gouw, J. A. de and Luxembourg, S. L.:  
975 Disjunct eddy covariance technique for trace gas flux measurements, *Geophys. Res. Lett.*,  
976 28(16), 3139–3142, doi:10.1029/2001GL012900, 2001.
- 977 Rinne, J., Markkanen, T., Ruuskanen, T. M., Petäjä, T., Keronen, P., Tang, M. J., Crowley, J.  
978 N., Rannik, Ü. and Vesala, T.: Effect of chemical degradation on fluxes of reactive  
979 compounds – a study with a stochastic Lagrangian transport model, *Atmos. Chem. Phys.*,  
980 12(11), 4843–4854, doi:10.5194/acp-12-4843-2012, 2012.
- 981 Schmidt, H., Derognat, C., Vautard, R. and Beekmann, M.: A comparison of simulated and  
982 observed ozone mixing ratios for the summer of 1998 in Western Europe, *Atmospheric*  
983 *Environment*, 35(36), 6277–6297, doi:10.1016/S1352-2310(01)00451-4, 2001.

- 984 Seufert, G., Bartzis, J., Bomboi, T., Ciccioli, P., Cieslik, S., Dlugi, R., Foster, P., Hewitt, C.  
985 N., Kesselmeier, J., Kotzias, D., Lenz, R., Manes, F., Pastor, R. P., Steinbrecher, R., Torres,  
986 L., Valentini, R. and Versino, B.: An overview of the Castelporziano experiments,  
987 *Atmospheric Environment*, 31, Supplement 1, 5–17, doi:10.1016/S1352-2310(97)00334-8,  
988 1997.
- 989 Silva, G. da, Graham, C. and Wang, Z.-F.: Unimolecular  $\beta$ -hydroxyperoxy radical  
990 decomposition with OH recycling in the photochemical oxidation of isoprene, *Environmental*  
991 *science & technology*, 44(1), 250–256, 2009.
- 992 Simon, V., Dumergues, L., Bouchou, P., Torres, L. and Lopez, A.: Isoprene emission rates  
993 and fluxes measured above a Mediterranean oak (*Quercus pubescens*) forest, *Atmospheric*  
994 *Research*, 74(1-4), 49–63, doi:10.1016/j.atmosres.2004.04.005, 2005.
- 995 Singer, W., Beauchamp, J., Herbig, J., Dunkl, J., Kohl, I. and Hansel, A.: Dynamic gas  
996 dilution system for accurate calibration of analytical instruments such as ptr-ms, in 3rd  
997 International Conference on Proton Transfer Reaction Mass Spectrometry and Its  
998 Applications, IUP Conference Series, pp. 232–234., 2007.
- 999 Spirig, C., Neftel, A., Ammann, C., Dommen, J., Grabmer, W., Thielmann, A., Schaub, A.,  
1000 Beauchamp, J., Wisthaler, A. and Hansel, A.: Eddy covariance flux measurements of biogenic  
1001 VOCs during ECHO 2003 using proton transfer reaction mass spectrometry, *Atmos. Chem.*  
1002 *Phys.*, 5(2), 465–481, doi:10.5194/acp-5-465-2005, 2005.
- 1003 Strong, C., Fuentes, J. D. and Baldocchi, D.: Reactive hydrocarbon flux footprints during  
1004 canopy senescence, *Agricultural and forest meteorology*, 127(3), 159–173, 2004.
- 1005 Stroud, C., Makar, P., Karl, T., Guenther, A., Geron, C., Turnipseed, A., Nemitz, E., Baker,  
1006 B., Potosnak, M. and Fuentes, J. D.: Role of canopy-scale photochemistry in modifying  
1007 biogenic-atmosphere exchange of reactive terpene species: Results from the CELTIC field  
1008 study, *Journal of Geophysical Research: Atmospheres*, 110(D17), n/a–n/a,  
1009 doi:10.1029/2005JD005775, 2005.
- 1010 Szopa, S., Foret, G., Menut, L. and Cozic, A.: Impact of large scale circulation on European  
1011 summer surface ozone and consequences for modelling forecast, *Atmospheric Environment*,  
1012 43(6), 1189–1195, doi:10.1016/j.atmosenv.2008.10.039, 2009.
- 1013 Taipale, R., Ruuskanen, T. M. and Rinne, J.: Lag time determination in DEC measurements  
1014 with PTR-MS, *Atmospheric Measurement Techniques*, 3(4), 853–862, doi:10.5194/amt-3-  
1015 853-2010, 2010.
- 1016 Taipale, R., Ruuskanen, T. M., Rinne, J., Kajos, M. K., Hakola, H., Pohja, T. and Kulmala,  
1017 M.: Technical Note: Quantitative long-term measurements of VOC concentrations by PTR-  
1018 MS – measurement, calibration, and volume mixing ratio calculation methods, *Atmos. Chem.*  
1019 *Phys.*, 8(22), 6681–6698, doi:10.5194/acp-8-6681-2008, 2008.
- 1020 Trainer, M., Williams, E. J., Parrish, D. D., Buhr, M. P., Allwine, E. J., Westberg, H. H.,  
1021 Fehsenfeld, F. C. and Liu, S. C.: Models and observations of the impact of natural  
1022 hydrocarbons on rural ozone, *Nature*, 329(6141), 705–707, doi:10.1038/329705a0, 1987.

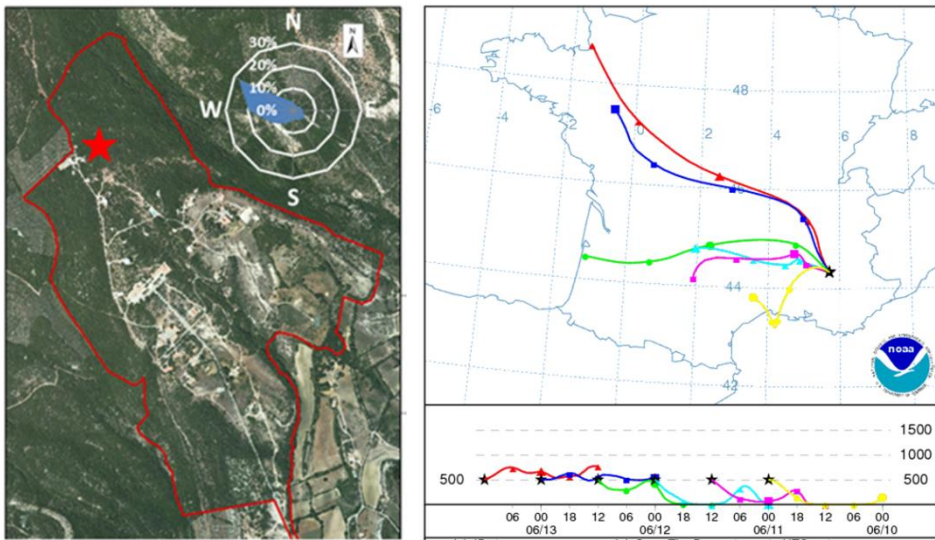
- 1023 Tsigaridis, K. and Kanakidou, M.: Global modelling of secondary organic aerosol in the  
1024 troposphere: a sensitivity analysis, *Atmospheric Chemistry and Physics*, 3(5), 1849–1869,  
1025 doi:10.5194/acp-3-1849-2003, 2003.
- 1026 Velentini, R., Greco, S., Seufert, G., Bertin, N., Ciccioli, P., Cecinato, A., Brancaleoni, E. and  
1027 Frattoni, M.: Fluxes of biogenic VOC from Mediterranean vegetation by trap enrichment  
1028 relaxed eddy accumulation, *Atmospheric Environment*, 31, Supplement 1, 229–238,  
1029 doi:10.1016/S1352-2310(97)00085-X, 1997.
- 1030 Wuebbles, D. J., Grant, K. E., Connell, P. S. and Penner, J. E.: The Role of Atmospheric  
1031 Chemistry in Climate Change, *JAPCA*, 39(1), 22–28, doi:10.1080/08940630.1989.10466502,  
1032 1989.
- 1033 Yuan, B., Hu, W. W., Shao, M., Wang, M., Chen, W. T., Lu, S. H., Zeng, L. M. and Hu, M.:  
1034 VOC emissions, evolutions and contributions to SOA formation at a receptor site in eastern  
1035 China, *Atmos. Chem. Phys.*, 13(17), 8815–8832, doi:10.5194/acp-13-8815-2013, 2013.
- 1036



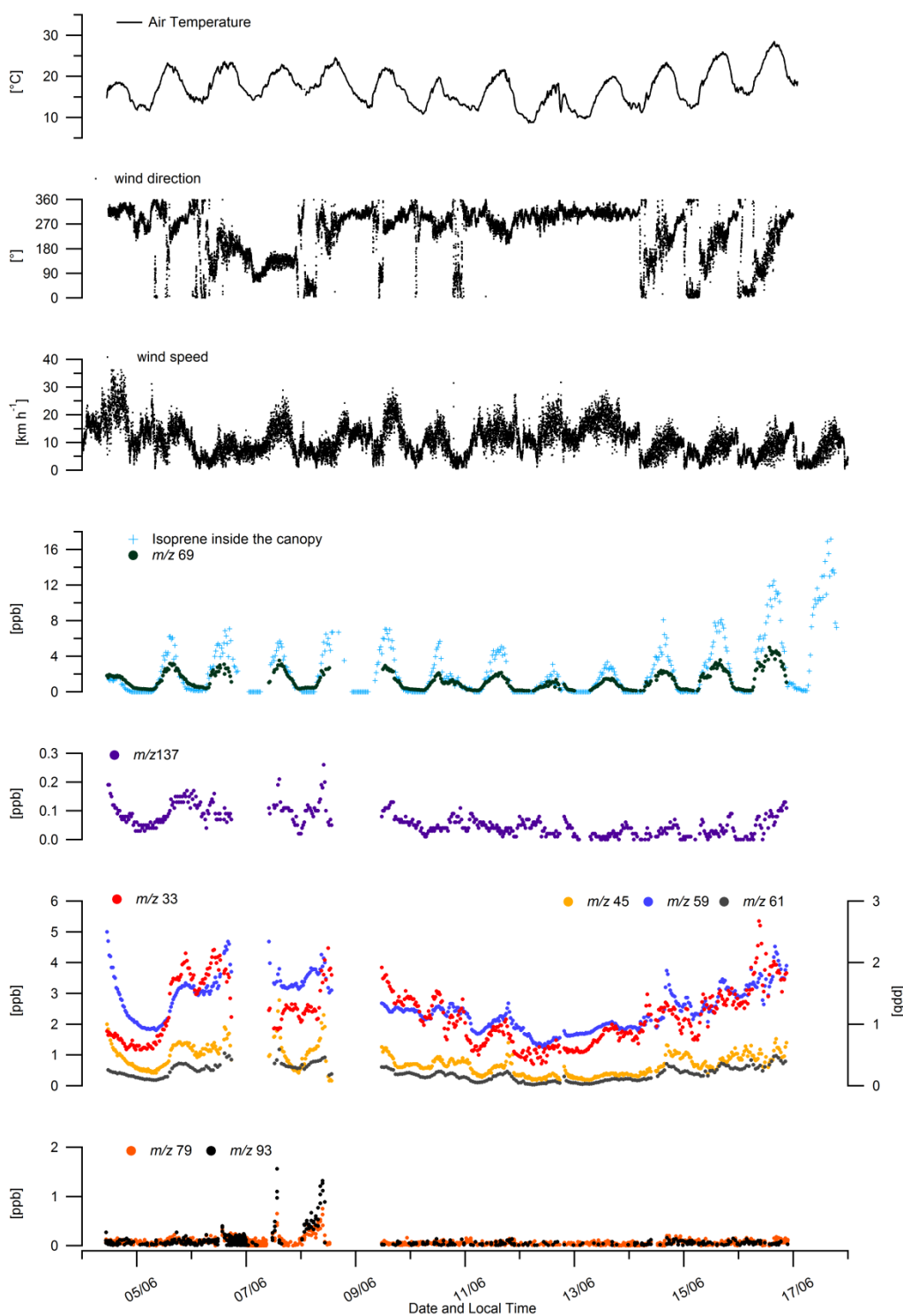
1037 **Figures**



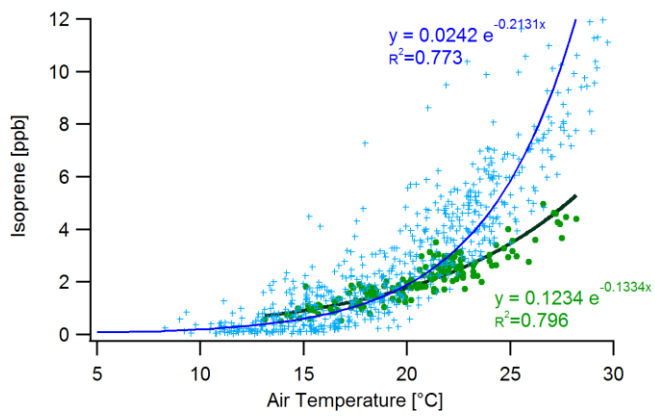
1038  
 1039 Figure 1. Seasonal variation of isoprene concentrations (3 m above ground) at the O<sub>3</sub>HP, May  
 1040 2011 to December 2011 and from April 2012 to June 2012. Measurement derived from  
 1041 cartridge samples and analysed by GC-MS.  
 1042



1043  
 1044 Figure 2. (left) Satellite photo of the Observatoire de Haute Provence. The red star represents  
 1045 the location of the measurements. Wind rose: Wind direction origins (%) from the 4<sup>th</sup> until the  
 1046 17<sup>th</sup> June 2012. (right) Location of the O<sub>3</sub>HP in the southeast of France. 24 hours duration  
 1047 backward trajectories ending at 00.00 UTC 14 Jun 12 (NOAA HYSPLIT MODEL)  
 1048



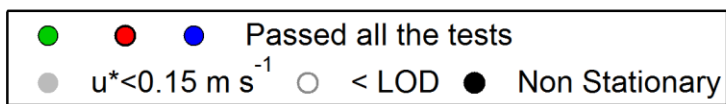
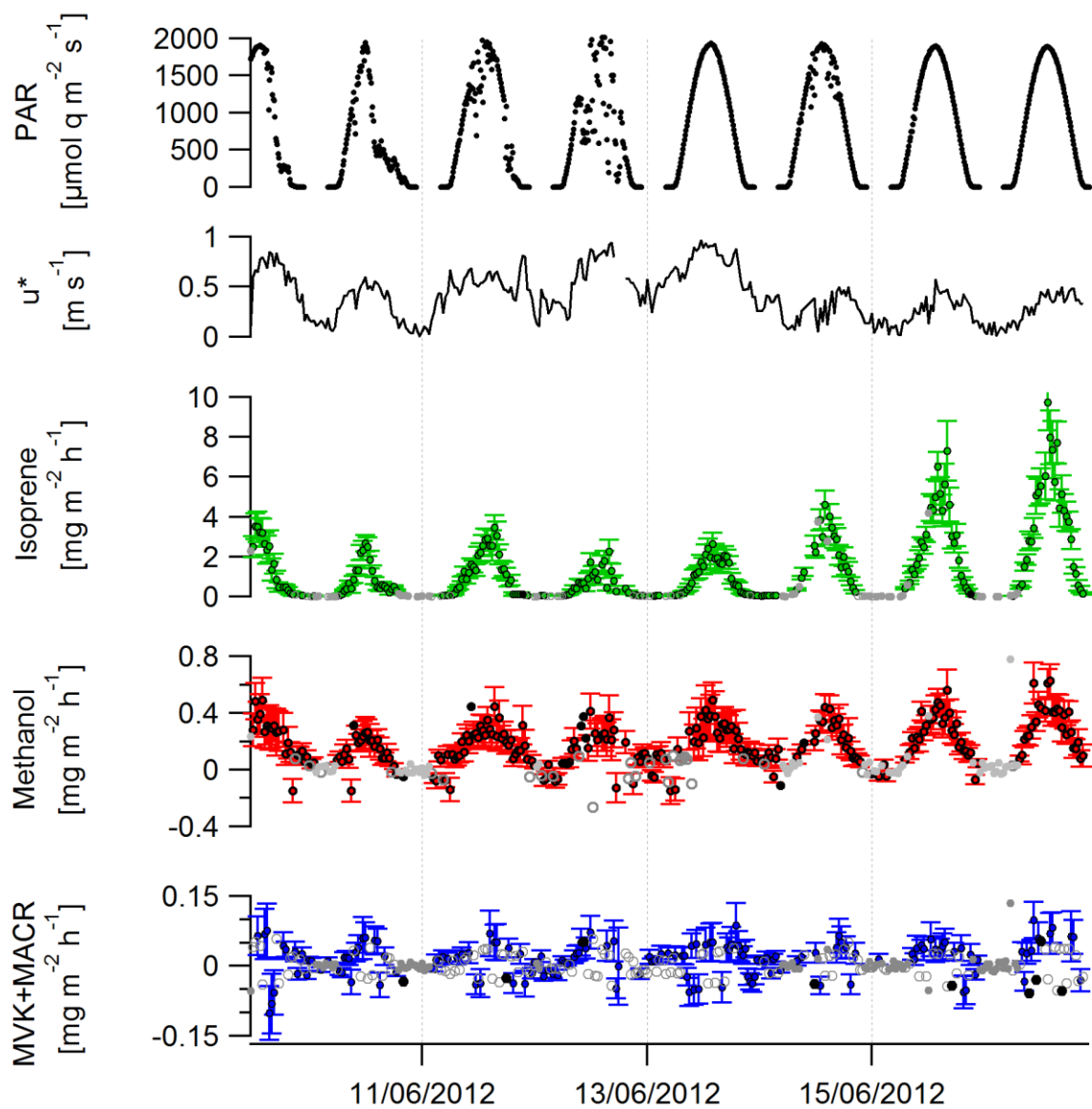
1049  
 1050 Figure 3. Time series of VOCs and meteorological parameters recorded from 4<sup>th</sup> to 16<sup>th</sup> June.  
 1051 Benzene ( $m/z$  79), toluene ( $m/z$  93), methanol ( $m/z$  33), acetaldehyde ( $m/z$  45), acetone ( $m/z$   
 1052 59), sum of acetic acid and glycoaldehyde ( $m/z$  61), total monoterpenes ( $m/z$  137) and isoprene  
 1053 ( $m/z$  69) were measured by PTR-MS above the canopy along with temperature and wind  
 1054 direction. Isoprene inside the canopy (2 m a.g.l) was measured by online GC-FID from 4<sup>th</sup> - 17<sup>th</sup>  
 1055 June.  
 1056



1057  
1058

1059 Figure 4. Relationship between daytime isoprene mixing ratios (ppbv) and air temperature (°C).  
1060 Datapoints and fit lines in green and blue correspond to measurements at 10 m and 2 m height  
1061 respectively.

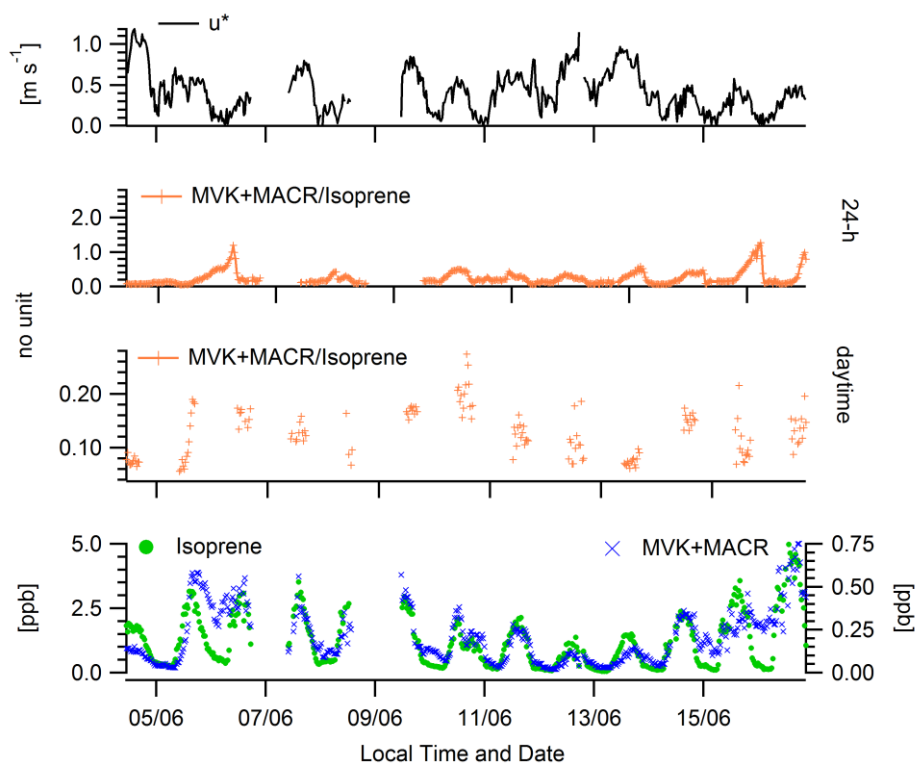
1062



1063  
1064

1065 Figure 5. Time series of MVK+MACR, methanol and isoprene fluxes along with friction  
1066 velocity and PAR measured above the canopy from the 4<sup>th</sup> June to the 16<sup>th</sup> of June. Flux error  
1067 bars show  $\pm$  standard deviation of the covariance for  $t_{lag}$  far away from the true lag (+150-  
1068 180 s).

1069

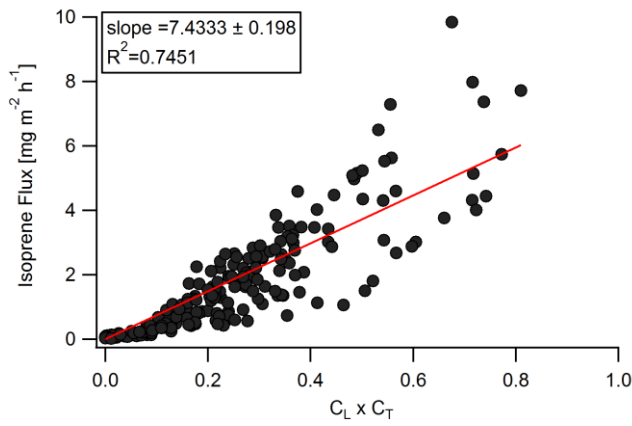


1070

1071

1072 Figure 6. Time series of MVK+MACR and isoprene concentrations, [MVK+MACR]/isoprene  
 1073 ratio (daytime dataset and whole dataset) along with friction velocity above the canopy of the  
 1074  $\text{O}_3\text{HP}$ .

1075



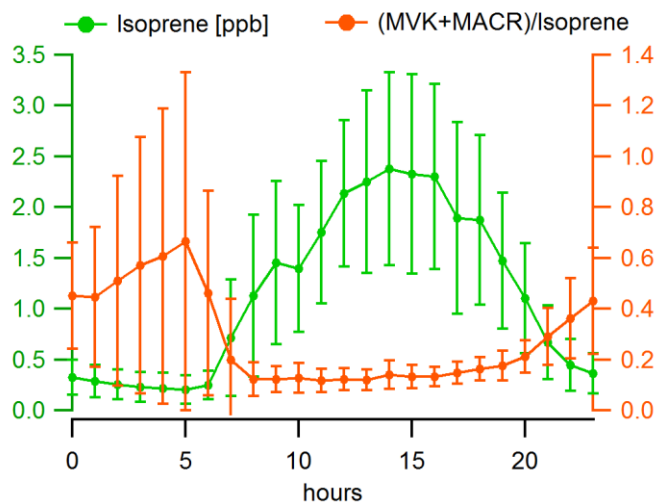
1076  
 1077 Figure 7. (Right) Isoprene fluxes against the combined temperature and light scaling factors  
 1078 ( $C_L$ ,  $C_T$ ):

$$C_T = e^{\frac{C_{T1}(T-T_S)}{RTT_S}} / \left( 1 + e^{\frac{C_{T2}(T-T_M)}{RTT_S}} \right)$$

1079 
$$C_L = \alpha C_{L1} L / \sqrt{(1 + a^2 L^2)}$$

1080 with  $L$ = Photosynthetically Active Radiation (PAR) in  $\mu\text{mol}(\text{photon}) \text{m}^{-2} \text{s}^{-1}$ ,  $a=0.0027$   
 1081  $\text{m}^2 \text{s} \mu\text{mol}^{-1}$ ,  $C_{L1}=1.066$  units,  $C_{T1}=95000 \text{ J mol}^{-1}$ ,  $C_{T2}=230000 \text{ J mol}^{-1}$ ,  
 1082  $T_S$ =standard temperature in Kelvin (303K to 30°C),  $T_M=314\text{K}$

1083



1084

1085 Figure 8. Averaged diel cycles of isoprene concentrations and [MVK+MACR]/isoprene ratio  
 1086 measured above the canopy of the O<sub>3</sub>HP from the 4<sup>th</sup> June to the 16<sup>th</sup> of June. Vertical bars do  
 1087 not show error but standard deviation to the mean value.

1088



Table 1. Normalized Sensitivities derived from the gas calibration. Limit of detections calculated as 2 times the standard deviation of the noise (ncps) divided by the normalised sensitivity.

VOC present in the calibration gas standard			
<i>m/z</i>	<i>Identified compound</i>	<i>S<sub>norm</sub> (ncps/ppbv)</i> <i>(dwell = 0.5 s)</i>	<i>LOD</i> <i>(ppbv)</i>
<b>33</b>	Methanol	17.2	0.31
<b>45</b>	Acetaldehyde	21.6	0.13
<b>59</b>	Acetone	22.9	0.05
<b>69</b>	Isoprene	9.8	0.07
<b>71</b>	Crotonaldehyde	27.4	0.03
<b>79</b>	Benzene	11.8	0.04
<b>93</b>	Toluene	12.4	0.07
<b>137</b>	$\alpha$ -Pinene	4.0	0.04

Table 2. Statistical summary of volume mixing ratios (ppbv) and fluxes of 12 targeted VOC above the canopy (10m) of the Oak Observatory of the Observatoire de Haute Provence.

<i>m/z</i>	Identified compound	Volume Mixing Ratios [ppbv]			Mean Flux [ $\text{mg m}^{-2} \text{h}^{-1}$ ]	
		Mean 24h-statistics	Mean (10:00-17:00)	Daily-Max	Mean (10:00-17:00)	Flux[ $\text{mg m}^{-2} \text{h}^{-1}$ ] Daily Max
<b>33</b>	Methanol	2.28	2.48	1.48-5.35	0.31	0.20-0.63
<b>45</b>	Acetaldehyde	0.38	0.42	0.20-1.39		
<b>59</b>	Acetone	1.28	1.35	0.88-2.45		
<b>69</b>	Isoprene	1.19	2.09	1.70-4.97	2.77	2.0-9.7
<b>71</b>	MVK+MACR	0.21	0.28	0.11-0.75	0.03	0.10
<b>*79</b>	Benzene	0.07	0.08	0.11-0.75		
<b>*93</b>	Toluene	0.05	0.09	0.13-1.37		
<b>137</b>	Monoterpens**	0.06	0.06	0.06-0.25		

\*Derived from 5-min hourly mass scans

Table 3. Quality assessment of isoprene, methanol and MVK+MACR fluxes

	Isoprene	Methanol	MVK+MACR
<b>Failure percentage among flux datapoints</b>			
<i>Quality Tests:</i>			
$u^* < 0.15 \text{ m s}^{-1}$	18%	19%	20%
F < LOD	11%	10%	37%
$\Delta s > 60\%$	1%	0%	3%
<b>Data that passed the quality assessment:</b>			
High quality Stationary data	94%	93%	81%
$\Delta s < 30\%$			
Low quality Stationary data	6%	7%	19%
$30\% < \Delta s < 60\%$			

	Site	Method	Daytime Fluxes [ $\text{mg m}^{-2} \text{h}^{-1}$ ]			Daytime VMR [ppbv]	Season	Reference
			Mean (Median)	Std conditions*	Max			
Mediterranean	Haute Provence, France downy oaks	DEC	2.77 (2.39)	7.43	9.85	2.09 (2.10) (max. 4.97)	Spring 2013	This study
	Haute-Provence, France downy oaks	DEC	- -		10.08	- -	Summer 2010	(Baghi et al., 2012)
	Western Italy, macchia ecosystem	DEC	(0.10/0.16/0.32 **)	0.43	0.29	(0.16/0.25/0.17)** (max. 0.60)	Spring 2007	(Davison et al., 2009b)
Tropical	Malaysia borneo oil plantation	DEC	9.71 (8.45)	7.80	28.94	13.10 (13.80) (max.21.40)	Spring 2008	(Misztal et al., 2011)
	Malaysia Rainforest	DEC	0.93 (0.46)	1.60	3.7	1.30 (1.00) (max. 3.40)	Spring-summer 2008	(Langford et al., 2010)
	Central Amazon mature lowland	REA	2.38±1.8		6.12	3.40±1.8 (3.2) (max. 6.60)	Summer 2001	(Kuhn et al., 2007)
	La Selva, Costa Rica oil tree	DEC	1.35	1.72	2,90	1.66 (max. 3.00)	Spring 2003	(Karl et al., 2004)
	Tabajos, Brazil terra firme	EC	-	2.40	2.00	- (max. 4.00)	Spring 2000	(Rinne et al., 2002)
Temperate	Central Massachusetts, mixed canopy	DEC	4.40	3.70-17.20	~13.50	- (max. >10.00)	Spring 2007	(McKinney et al., 2011)
	Germany mixed deciduous: beech, oak	DEC	3.38	2.88	10.8	- (max. 4.00)	Summer 2003	(Spirig et al., 2005)
	Eastern Belgium mixed coniferous species	DEC	-	2.01-3.28	7.06	- (max. <1.50)	Summer 2009	Laffineur et al., 2011

\* Fluxes normalized to standard conditions:  $1000 \mu\text{mol m}^{-2} \text{s}^{-1}$ ,  $30^\circ\text{C}$

\*\* Values correspond to fluxes measured using the DEC method using three different proton transfer reaction mass spectrometers

Table 4. Non exhaustive overview of above-canopy isoprene fluxes and volume mixing ratios in different ecosystems of the world